

Electronic Thesis and Dissertation Repository

---

7-21-2022 1:00 PM

## Acidic pH Environment Alters Cell Death and Regulates AIF Translocation in Endothelial Cells

Laura Xu, *The University of Western Ontario*

Supervisor: Zhang, Zhu-Xu, *The University of Western Ontario*

A thesis submitted in partial fulfillment of the requirements for the Master of Science degree in Pathology and Laboratory Medicine

© Laura Xu 2022

Follow this and additional works at: <https://ir.lib.uwo.ca/etd>



Part of the [Pathology Commons](#)

---

### Recommended Citation

Xu, Laura, "Acidic pH Environment Alters Cell Death and Regulates AIF Translocation in Endothelial Cells" (2022). *Electronic Thesis and Dissertation Repository*. 8653.

<https://ir.lib.uwo.ca/etd/8653>

This Dissertation/Thesis is brought to you for free and open access by Scholarship@Western. It has been accepted for inclusion in Electronic Thesis and Dissertation Repository by an authorized administrator of Scholarship@Western. For more information, please contact [wlsadmin@uwo.ca](mailto:wlsadmin@uwo.ca).

## Abstract

Cardiac transplantations are the golden standard treatment for end-stage heart failure but issues like ischemia-reperfusion injury (IRI) and graft rejection persist. Prolonged ischemia induces anaerobic metabolism, lactic acid accumulation, and intracellular acidosis. IRI is associated with programmed cell death, of which necroptosis is significant. We have shown that in hypoxia-reoxygenation, targeting necroptosis prevents murine microvascular endothelial cell (MVEC) death through cyclophilin D inhibition *in vitro* and apoptosis-inducing factor (AIF) is implicated in DNA damage. Here, we investigated AIF and the impact of acidic pH on cell death. Acidic pH conditions altered MVEC necroptosis to an apoptosis-like pattern. AIF nuclear translocation and DNA fragmentation increased. Endonuclease G did not translocate into the nucleus, suggesting other nucleases may be involved in DNA fragmentation. PARP-1 regulates AIF translocation and DNA fragmentation. Clarifying the mechanisms underlying ischemia and the acidic cellular environment may lead to therapeutic strategies preventing IRI and cardiac transplant graft rejection.

## Keywords

Apoptosis-inducing factor (AIF), pH, necroptosis, apoptosis, endothelial cells, ischemia, nuclear translocation, nuclear damage, reperfusion, acidosis

## Summary for Lay Audience

Organ transplantation is an important treatment for patients with end-stage organ disease, including people with heart failure. However, transplantations can cause organ damage through limiting blood supply. This reduction in blood oxygen can cause the organ environment to be acidic. Despite advances in organ storage and transportation, there has been a lack of strategies that look to reduce cell death in ischemic injury. Thus, it is important to understand the pathways of cell death that are involved in ischemia in acidic conditions. Necroptosis is a form of cell death that has been found to be involved in transplantations and is believed to promote inflammatory injury, triggering an immune response against the transplanted organ. The specific mechanisms of necroptosis in the context of ischemia and transplantation are unclear, but current research has implicated the mitochondria and related molecules. This includes the focus of this project, apoptosis-inducing factor (AIF), which has been shown to move from the mitochondria to the nucleus facilitating DNA damage under conditions of ischemic stress. The goal of this project was to determine the role of AIF in a cardiac transplantation model. Chemical reagents and genetic inhibition were used to stimulate cell death and prevent AIF from performing its role within the cell. Cell death was reduced in acidic conditions, but the action of AIF was not blocked. It is hoped that by better understanding these cell death pathways, potential clinical targets can be studied to improve the organ transplantation process and long-term success.

## Co-Authorship Statement

The following individuals contributed to this research project:

- Patrick McLeod at the Matthew Mailing Centre for Translational Transplant Studies in London Health Sciences Centre performed part of the death assays and immunocytochemistry experiments.
- Xuyan Huang at the Matthew Mailing Centre for Translational Transplant Studies in London Health Sciences Centre isolated and ran DNA gel electrophoresis following death assays for analysis.
- Haitao Lu in the Department of Pathology and Laboratory Medicine at the University of Western Ontario performed western blots on cell samples.

## Acknowledgments

I would like to thank my supervisor, Dr. Zhu-Xu Zhang, for his support and guidance during the course of my master's degree. I am also grateful for the expertise and help that I received from Patrick McLeod and Xuyan Huang for teaching me basic laboratory techniques and for troubleshooting and refining many of my experiments. Thank you to my lab members, Haitao Lu, Connar Lee, and Jeffrey Min, for their friendship as colleagues and for their advice. I would also like to thank the current and former administrative staff at the Matthew Mailing Centre for their support: Dr. Jacqueline Arp, Katherine Branton, Catherine Fraser, and Pamela Gardner. Furthermore, I would like to acknowledge my advisory committee members, Dr. Biao (Francis) Feng and Dr. Martin Duennwald for their insights and guidance throughout my studies. Finally, I am forever grateful for my family for their constant support and encouragement.

# Table of Contents

Abstract.....	ii
Summary for Lay Audience.....	iii
Co-Authorship Statement.....	iv
Acknowledgments.....	v
Table of Contents.....	vi
List of Figures.....	ix
List of Abbreviations.....	x
Chapter 1.....	1
1 Introduction.....	1
1.1 Current Challenges in Cardiac Transplantation.....	1
1.1.1 Short Term Complications Following Cardiac Transplantation.....	1
1.1.2 Long Term Complications Following Cardiac Transplantation.....	3
1.2 Ischemia-Reperfusion Injury in Cardiac Transplantation.....	4
1.2.1 Molecular Mechanisms of Ischemic Injury.....	5
1.2.2 Molecular Mechanism of Reperfusion Injury.....	7
1.2.3 Inflammatory Response in Ischemia-Reperfusion Injury.....	8
1.2.4 The Role of Endothelial Cells in IRI.....	9
1.3 Endothelial Cells in Cardiac Transplantation.....	9
1.4 Endothelial Cell Death Pathways.....	10
1.4.1 Apoptosis.....	11
1.4.2 Necroptosis.....	12
1.5 Mitochondrial Permeability Transition Pore.....	17
1.6 Apoptosis-Inducing Factor.....	17
1.7 Study Rationale.....	18

1.8 Hypothesis.....	19
1.9 Study Aims.....	19
Chapter 2.....	20
2 Materials and Methods.....	20
2.1 Mice .....	20
2.2 Endothelial Cell Culture .....	20
2.3 Cell Death Assay.....	21
2.3.1 pH Adjustment of Cell Media.....	21
2.3.2 Real-Time Cell Death via IncuCyte.....	21
2.3.3 Cell Death and Apoptosis Quantification with Flow Cytometry .....	22
2.4 Immunocytochemistry .....	23
2.4.1 Quantification of Positive Nuclear Translocation.....	24
2.5 RNA Interference Silencing.....	24
2.6 RT-qPCR.....	25
2.7 Western Blots.....	25
2.8 DNA Gel Analysis .....	27
2.9 Statistical Analysis.....	27
Chapter 3.....	29
3 Results .....	29
3.1 Acidic pH Inhibits TNF- $\alpha$ -Mediated Necroptosis in Endothelial Cells .....	29
3.2 RIPK1 Function Is Unchanged at Acidic Conditions .....	35
3.3 Nuclear Translocation of AIF in Endothelial Cells is pH-Dependent .....	39
3.4 Endonuclease G Does Not Participate in Translocation of AIF at Acidic Conditions.....	48
3.5 AIF Induces DNA Fragmentation in Endothelial Cells at Acidic Conditions.....	51
3.6 AIF Silencing Did Not Prevent Cell Death at Acidic pH.....	53

3.7	Cyclophilin A is Modestly Involved in Endothelial Cell Death at Acidic Conditions .....	58
3.8	Parthanatos May Be Involved in Endothelial Cell Death at Acidic Conditions ...	60
	Chapter 4.....	64
4	Discussion .....	64
4.1	Study Summary.....	64
4.1.1	The Endothelium in Organ Transplantation .....	65
4.1.2	Necroptosis in IRI and Organ Transplantation .....	65
4.1.3	The Impact of Acidic pH on Necroptosis .....	66
4.1.4	Acid-Induced Cell Death Upregulates AIF Nuclear Translocation .....	67
4.2	Future Directions .....	68
4.3	Limitations .....	69
4.4	Conclusion and Study Significance .....	70
	References.....	72
	Curriculum Vitae .....	88



# List of Figures

Figure 1: Cellular biology of ischemia .....	6
Figure 2: Cellular biology of reperfusion .....	8
Figure 3: Pathway of apoptosis vs. necroptosis .....	14
Figure 4: Downstream pathway of necroptosis .....	15
Figure 5: Apoptosis and necroptosis in endothelial cells at pH 7.4.....	30
Figure 6: Inhibition of necroptosis in endothelial cells at pH 6.5.....	32
Figure 7: Cell death at pH 6.5 mainly leads to apoptosis in endothelial cells .....	34
Figure 8: RIPK1 is not altered at acidic pH.....	38
Figure 9: Nuclear translocation of AIF in endothelial cells is pH-dependent .....	44
Figure 10: PARP-1 and CypA inhibition reduces nuclear translocation of AIF at acidic pH conditions.....	47
Figure 11: Endonuclease G does not translocate into the nucleus at pH 7.4 and 6.5 .....	50
Figure 12: Effects of PARP-1 and CypA inhibitors on DNA fragmentation at acidic pH conditions.....	52
Figure 13: Confirmation of siRNA-induced silencing of <i>Aifm1</i> in endothelial cells .....	54
Figure 14: AIF siRNA-induced silencing increased cell death .....	57
Figure 15: Cyclophilin A is modestly involved in endothelial cell death at acidic pH conditions.....	59
Figure 16: Parthanatos may contribute to endothelial cell death.....	62
Figure 17: Proposed mechanism of necroptosis in acidic pH conditions .....	68

## List of Abbreviations

**3-ABA:** 3-aminobenzamide

**AIF:** apoptosis-inducing factor

**ADP-ribose:** adenosine diphosphate ribose

**ATP:** adenosine triphosphate

**BSA:** bovine serum albumin

**CAV:** cardiac allograft vasculopathy

**cIAP1/2:** cellular inhibitors of apoptosis 1 and 2

**CypA:** cyclophilin A

**CypD:** cyclophilin D

**DIABLO:** direct IAP binding protein with low pI

**DMEM:** Dulbecco's modified eagle medium

**DPBS:** Dulbecco's phosphate-buffered saline

**DPBS-T:** Dulbecco's phosphate-buffered saline with 0.1% Tween-20

**EndoG:** endonuclease G

**HLA:** human leukocyte antigen

**IAP:** inhibitor of apoptosis protein

**ICC:** immunocytochemistry

**IETD:** Z-Ile-Glu-Thr-Asp-fluoromethyl ketone

**IRI:** ischemia-reperfusion injury

**MIF:** macrophage migration inhibitor factor

**MLKL**: mixed lineage kinase domain-like protein

**MPTP**: mitochondrial permeability transition pore

**MVEC**: mouse microvascular endothelial cells

**Nec-1s**: necrostatin-1 stable

**PARP-1**: poly (ADP-ribose) polymerase 1

**PCD**: programmed cell death

**PCR**: polymerase chain reaction

**p-RIPK1**: phosphorylated RIPK1

**PVDF**: polyvinylidene fluoride

**RIPK1**: receptor-interacting protein kinase 1

**SMAC**: second mitochondrial activator of caspases

**hTNF- $\alpha$** : human tumor necrosis factor alpha

**TNF- $\alpha$** : tumor necrosis factor alpha

**TNFR1**: tumor necrosis factor receptor 1

**TX100**: Triton™ X-100

**WT**: wild-type

## Chapter 1

### 1 Introduction

#### 1.1 Current Challenges in Cardiac Transplantation

Heart failure has become increasingly prevalent in an aging population with complex medical conditions, and accounts for considerable mortality and morbidity worldwide<sup>1,2</sup>. As of 2017, around 64.34 million individuals were estimated to suffer from heart failure worldwide, which is characterized by dyspnea or limited exertion due to either impairments in ventricular filling or ejection of blood from the heart<sup>3,4</sup>. For patients with persisting and advanced chronic heart failure despite medical management, heart transplantation remains one of the best treatments and has resulted in an almost 90% one-year survival rate since the first heart transplant was performed in 1967<sup>5-7</sup>. However, long-term and short-term challenges in cardiac transplantation are still present, which negatively impacts patient mortality and morbidity. Most potential donor hearts are non-viable for transplantations due to ischemic injury, severely limiting the availability of donor organs<sup>8</sup>. There is also a mismatch between supply and demand, where the number of patients with end-stage heart failure has been increasing but the supply of donor organs has remained constant<sup>6,8</sup>. Patients for heart transplantations are now older ( $\geq 65$  years of age), may require mechanical support, and present with circulating antibodies, known as sensitization, which can limit transplantation success<sup>6,9</sup>. Early complications after cardiac transplantations can include primary graft dysfunction, acute right ventricular failure, and conduction abnormalities<sup>5,6,10</sup>. Moreover, issues can arise in the long-term after a transplantation, including cardiac allograft vasculopathy, malignancy, and infection due to immunosuppression<sup>5,6,10</sup>.

##### 1.1.1 Short Term Complications Following Cardiac Transplantation

Primary graft dysfunction occurs in 10-20% of heart transplantations and is the most common cause of mortality, up to 30%, in the first month following the transplant<sup>6,11-13</sup>. It is defined as a condition where the transplanted heart cannot meet the circulatory demands of the recipient<sup>13</sup>. Patients who have moderate or severe primary graft

dysfunction have been shown to be at increased risk of mortality during the first 90 days following transplantation compared to those with mild or no primary graft dysfunction<sup>12,14</sup>. Although the one-month mortality following cardiac transplantation is 8%, primary graft dysfunction is involved in 39% of those deaths<sup>11</sup>.

Acute right ventricular failure occurs in 2-3% of patients after transplantation but with a greater than 50% mortality rate<sup>6</sup>. There are multiple potential causes of the condition which are not limited to prolonged ischemia-reperfusion time, elevated pulmonary vascular resistance, and donor size mismatch<sup>6,11</sup>.

Conduction abnormalities are an inevitable aspect of the heart transplant due to the denervation of the donor heart, cutting off efferent and afferent nerve signalling in the organ.<sup>6,15</sup> The loss of parasympathetic and sympathetic efferent signals impacts baroreceptor response<sup>6,15</sup>. If hypotension is present, the lack of activation from the baroreceptors of the sympathetic nervous system will lead to insufficient increase of cardiac output<sup>6</sup>. This will contribute to hemodynamic instability following the transplant along with abnormal cardiac output responses to exercise in response to the denervation<sup>15</sup>.

The rejection of the transplanted organ, otherwise known as cardiac allograft rejection, can occur due to the pathological changes induced by ischemia-reperfusion injury (IRI) and the inflammatory response. There are three types of rejection that can present following transplant – hyperacute rejection, acute cellular rejection, and antibody-mediated rejection<sup>6,12</sup>.

Hyperacute rejection happens during the transplant procedure once the donor heart is exposed to the recipient's red blood cells<sup>6</sup>. It is mediated by pre-formed antibodies against the donor allograft and donor human leukocyte antigens, leading to widespread complement activation, hemorrhage, and thrombosis within the graft<sup>6,16,17</sup>. Although it has a high mortality rate, the presentation of hyperacute rejection is now limited due to cross-matching of blood types and the use of panel reactive antibodies<sup>6,16</sup>. It cannot be prevented with immunosuppressive drugs but may not occur in children under 2 years of age due to the still-developing immune system<sup>18,19</sup>.

Acute cellular rejection is caused by T-cells, usually in the first year following the transplant<sup>6,10,12</sup>. The T-cells of the recipient recognizes the donor's human leukocyte antigen (HLA) expressed on donor-derived antigen presenting cells or the presentation of donor-derived peptides on recipient antigen-presenting cells<sup>6,12,17</sup>. When this occurs, there is an amplification of the immune response by effector T cells, antibodies by B cells, and involvement of the macrophages<sup>17</sup>. It is characterized by leukocyte infiltration and myocyte damage in the heart. Acute cellular rejection has been associated with increased expression of the HLA class I and II antigens along with infiltration of CD8<sup>+</sup> T-cells<sup>20</sup>. CD4<sup>+</sup> T-cells recruit effector cells such as CD8<sup>+</sup> T-cells, macrophages, natural killer cells, and B cells<sup>16,20,21</sup>. Antigen presenting cells, specifically dendritic cells, move into the lymphoid follicles of the recipient to present peptides which leads to rejection by the adaptive immune system<sup>21</sup>.

Antibody-mediated (humoral) rejection occurs through complement system activation by recipient antibodies directed against the donor HLA on the endothelium<sup>6,22,23</sup>. This rejection occurs in 10-20% of patients with a mortality rate of 8%<sup>6,24</sup>. The donor antigens and recipient antibodies form a membrane attack complex (MAC), resulting in vascular and endothelial injury<sup>6</sup>.

### 1.1.2 Long Term Complications Following Cardiac Transplantation

Cardiac allograft vasculopathy (CAV) is the most common cause of long-term mortality in heart transplant patients, affecting almost 50% of patients ten years following transplantation<sup>12,25</sup>. Risk factors can include donor and recipient age, hypertension, diabetes mellitus, dyslipidemia, cytomegalovirus, and mismatch of body size and/or HLA<sup>12,21</sup>. Clinical presentation of CAV can vary by patient, but diagnosis is hard to accomplish based on signs and symptoms because of the denervation of the transplanted heart<sup>21</sup>. An early determinant of CAV is endothelial injury and dysfunction<sup>26</sup>. The major aspect of CAV is progressive diffuse thickening of the arterial intima with concentric fibrous hyperplasia in the epicardial and intramyocardial arteries of the transplanted heart<sup>27,28</sup>. Atypical clinical presentation such as heart failure, arrhythmias, or sudden cardiac death can also point to CAV<sup>6,29</sup>.

Malignancy can be a risk following cardiac transplantation, especially skin cancers and lymphomas, which impact 19.8% and 1.8% of patients respectively within 10 years after the transplant<sup>6,30</sup>. Patients with organ transplants have a 3-4-fold likelihood of developing carcinoma compared to the general population<sup>30,31</sup>. This results from the need for immunosuppression, causing impaired immune responses against malignant cells and oncogenic viruses<sup>31</sup>. The risk for malignancies also increases with time following the transplant<sup>30</sup>. The use of proliferative signal inhibitors may be used to provide immunosuppression but also prevent cancers due to their anti-neoplastic properties<sup>30,31</sup>.

One inevitable consequence of cardiac transplantation is the need for immunosuppression to prevent graft rejection and improve patient survival. Usually this consists of a triple-therapy regimen involving calcineurin inhibitors, purine synthesis inhibitors, and corticosteroids<sup>6,31</sup>. Proliferation signal inhibitors can also be added in the case of poor renal function or CAV<sup>6,31</sup>. Corticosteroids can inhibit various types of leukocytes and block cytokine gene expression through inhibition of two transcription factors, activator protein-1 (AP-1) and nuclear factor- $\kappa$ B<sup>32</sup>. Lymphocytes and non-lymphocytes are affected which decreases inflammatory responses, interfering with major histocompatibility complex (MHC) class II molecules expression on antigen-presenting cells through the suppression of interferon  $\gamma$ , interleukin-1, interleukin-6, tumor necrosis factor alpha, prostaglandins, and leukotrienes<sup>17</sup>.

## 1.2 Ischemia-Reperfusion Injury in Cardiac Transplantation

Ischemia-reperfusion injury (IRI) is a major concern for the success of the transplant and graft function<sup>8,33,34</sup>. It is a multi-factorial issue which can negatively impact graft survival and lead to graft rejection<sup>34</sup>. Currently, static cold storage in preservation solutions is the standard method to reduce ischemic injury to cardiac grafts<sup>35</sup>. Furthermore, donor ischemia times are important to consider as increases are associated with primary graft dysfunction and patient survival times<sup>35</sup>. Based on clinical guidelines, the general threshold for donor heart ischemia time is around four hours. Hearts with an ischemic time over 4-6 hours are associated with increased risk of primary graft failure, acute cellular rejection, and 1 year mortality following transplant and are highly discouraged<sup>11,35-37</sup>. Several studies have also shown that there is greater tolerance for

prolonged ischemia using grafts from younger donors, with one study finding that the long-term outcomes for patients receiving older hearts ( $\geq 50$  years) and patients receiving younger hearts ( $< 50$  years) were similar when ischemia times were less than 2 hours long, but patients receiving older hearts with ischemia times greater than 2 hours had poorer 5-year outcomes than the matched group of patients receiving younger hearts<sup>38,39</sup>.

### 1.2.1 Molecular Mechanisms of Ischemic Injury

Ischemia occurs in the donated organ because of the cessation or limitation of blood flow, leading to low levels of oxygen, glucose, and substances for metabolism throughout the organ (Figure 1)<sup>33,40</sup>. The reduced oxygen availability induces a change from fatty acid metabolism in cardiomyocytes and endothelial cells into anaerobic respiration, causing lactic acid accumulation and intracellular acidosis<sup>8,40,41</sup>. A negative feedback loop occurs as glycogen is broken down through anaerobic glycolysis to produce lactic acid and ATP, where the decrease in pH inhibits ATP production further<sup>33,42</sup>. The lactic acidosis causes a significant drop in the extracellular and intracellular pH as low as 6.0 to 6.5<sup>8</sup>. As a result of the acidosis,  $\text{Na}^+/\text{H}^+$  membrane pump becomes more active to offset the acidic environment<sup>43</sup>. The increase in sodium ions within the cells increases  $\text{Na}^+/\text{Ca}^{2+}$  exchanger activity, drawing water into the cells to result in cellular edema<sup>33</sup>. The loss of adenosine triphosphate (ATP) contributes to dysfunction of ATP-dependent calcium pumps, leading to an influx of calcium ions in the cytoplasm and extracellular spaces<sup>33,40</sup>. Degradation of ATP produces adenosine, inosine, hypoxanthine, and xanthine molecules. The accumulation of calcium ions activates calpains and calcium-dependent kinases, resulting in damage to cellular structures. Phospholipases are also activated in the cells, which leads to degradation of membrane lipids and an increase in fatty acids<sup>33</sup>.

In the context of transplantations, ischemia occurs in two phases, called warm ischemia and cold ischemia<sup>13,36</sup>. During warm ischemia, the blood supply of the donor organ is stopped. Cold ischemia then occurs by flushing the organ with a cold preservation solution and stored at 4°C during transportation. Warm ischemia then briefly re-occurs prior to the graft being transplanted into the recipient and before blood flow is re-established<sup>13,36</sup>. Previous studies have shown that both intracellular and extracellular acidic pH during the start of ischemia impacts perfusion pressure levels in the tissue<sup>44</sup>.



Furthermore, cardiac contractability is also reduced during ischemia due to the pH change in both aerobic and anaerobic regions of the organ<sup>45</sup>. In a previous study published by our group, we were able to show that in mouse microvascular endothelial cells (MVECs), extracellular pH changes also altered the intracellular pH using a pH sensitive dye which increases in fluorescence when the pH becomes acidic<sup>46</sup>.

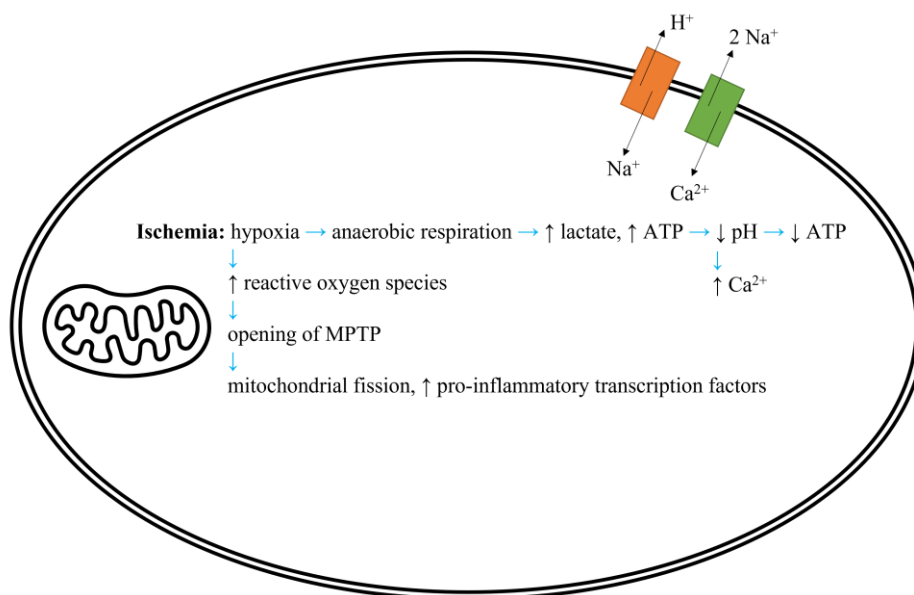


**Figure 1: Cellular biology of ischemia**

The molecular mechanisms of ischemia and physiological changes that occur within the cell. The shift to anaerobic respiration leads to increases in lactic acid, resulting in intracellular acidosis. The greatest change during ischemia is the overall decreased production of intracellular ATP due to the acidification of the immediate surrounding microenvironment. This causes energy-dependent systems such as ion channels to fail, leading to intracellular accumulation of sodium and calcium ions. Overall, the changes in ionic homeostasis and energy-dependent systems can lead to cell death<sup>33,40</sup>.

### 1.2.2 Molecular Mechanism of Reperfusion Injury

The restoration of blood flow to donated organs following transplantation into the recipient is called reperfusion<sup>47</sup>. Although the return of blood flow to the organs can save ischemic tissues, it also paradoxically causes further damage to the organ and impacts its viability<sup>33,47,48</sup>. During this time, the accumulated hydrogen ions become washed out from the cells, allowing the intracellular pH of the cells to increase, returning to physiological pH (Figure 2)<sup>33,40</sup>. However, the movement of protons out of the cell causes an increase in the proton gradient across the cell membrane, which further enhances the levels of calcium within the cells. Furthermore, the xanthine molecules formed during ischemia react to the incoming molecular oxygen during reperfusion and leads to superoxide anions, which break down into hydrogen peroxide and hydroxyl radicals<sup>33</sup>. There is an increase in reactive oxygen species (ROS) generation because ischemic cells have a lower concentration of antioxidative agents<sup>49</sup>. The xanthine oxidase system, reduced nicotinamide adenine dinucleotide phosphate (NADPH) oxidase system, mitochondrial electron transport chain (ETC), and uncoupled nitric oxide synthase (NOS) system are the major sources of ROS during reperfusion<sup>49,50</sup>. The generated ROS attack lipid structures of the cell membranes and release proinflammatory molecules that disrupt membrane permeability and cause endothelial dysfunction and DNA damage<sup>33,40</sup>. Reperfusion causes neutrophils, CD4<sup>+</sup> T lymphocytes, and circulating platelets to move into the vascular space, leading to further ROS production along with production of inflammatory mediators, causing tissue damage<sup>48</sup>. It also opens the mitochondrial permeability transition pores (MPTPs) in the inner mitochondrial membrane, increasing calcium levels in the mitochondria, leading to membrane rupture and cell death of cardiomyocytes and endothelial cells<sup>42,51-54</sup>.

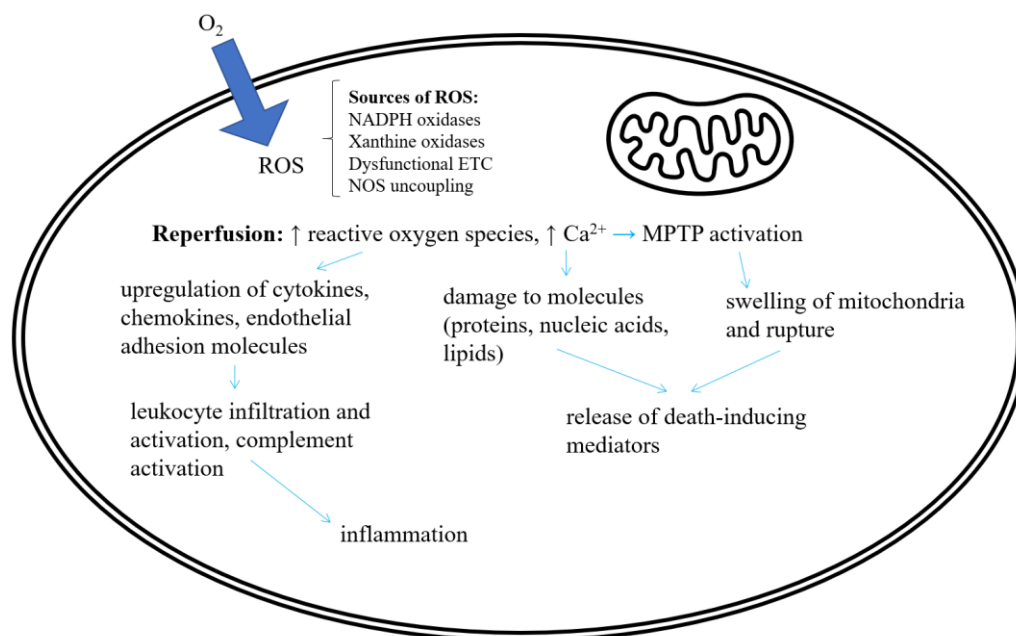


**Figure 2: Cellular biology of reperfusion**

During reperfusion, the impaired mitochondrial and cellular enzymes, dysfunction of the electron transport chain and reduced reactive oxygen species (ROS) scavenging leads to an increase in ROS within the cells<sup>33</sup>. This causes damage to lipids and DNA and also induces opening of the MPTP<sup>48</sup>. This uncouples oxidative phosphorylation and leads to the swelling of the mitochondria, causing a further decrease in ATP and the release of mitochondrial mediators of programmed cell death (PCD)<sup>33,40</sup>.

### 1.2.3 Inflammatory Response in Ischemia-Reperfusion Injury

The pathological changes which occur in ischemia-reperfusion injury can lead to an inflammatory response in the allograft which affects survival and function by activating the innate immune response following the transplant. Immune cells such as leukocytes and T cells are moved to the site of injury while the release of inflammatory molecules mediates local and remote tissue damage<sup>42,55</sup>. Reactive oxygen species that present during reperfusion are a major contributor to the inflammatory response that occurs and are produced from macrophages, endothelial cells, and immune cells<sup>56</sup>. When this happens, the insufficient numbers of endogenous free radical scavenging enzymes promote mitochondrial dysfunction and inflammation<sup>55</sup>. This leads to injury and cell death from

regulated cell death pathways, releasing damage-associated molecule patterns (DAMPs) and cytokines such as high mobility group box 1 (HMGB1)<sup>56</sup>. The DAMPs released by injured and necrotic cells are recognized by pattern recognition receptors (PRRs) expressed by innate immune cells and endothelial cells<sup>42,56</sup>. This causes the production of pro-inflammatory chemokines and cytokines, promoting leukocyte infiltration and complement system activation, further activating the innate immune system<sup>42</sup>.

#### 1.2.4 The Role of Endothelial Cells in IRI

The endothelium is a source of nitric oxide during IRI. Typically, in healthy conditions, nitric oxide has been shown to cause vasodilation, which can be protective during IRI by allowing for increased oxygen consumption, platelet and leukocyte adhesion, and scavenging of free radicals<sup>40</sup>. The endothelium can also help to provide vasoactive substances and expresses cytokines, chemokines, and adhesion molecules to combat the pathological changes during IRI<sup>40</sup>. This activation of the endothelium at the site of injury during reperfusion can cause tissue infiltration by neutrophils and platelets, increasing pro-inflammatory cytokines and adhesion molecules present in the vessels<sup>40</sup>.

### 1.3 Endothelial Cells in Cardiac Transplantation

The endothelium is a thin membrane of endothelial cells that line the inside of blood vessels and the heart<sup>40,57,58</sup>. Endothelial cells are important in maintaining organ homeostasis<sup>40,57,58</sup>. Within the heart, some of the functions of the endothelium are regulating blood flow, vascular permeability, and maintaining vessel structure<sup>57-60</sup>. The endothelium regulates vascular tone through production of molecules such as nitric oxide, cytokines, and prostaglandins<sup>61</sup>. However, during endothelial dysfunction, there is an imbalance between the vasodilatory and vasoconstrictive activities of the endothelium mediated by oxidative stress, which can lead to or further exacerbate heart failure<sup>61-63</sup>. This can occur during reperfusion in cardiac transplantation when there is an increase in ROS following ischemia<sup>56</sup>. Furthermore, endothelial cells are considered antigen-presenting cells, expressing the antigens which are recognized by immune cells<sup>64</sup>. As a result, in transplantation, endothelial cells are a target for the host immune system to

distinguish between self and non-self, where the immune response may lead to allograft rejection<sup>64,65</sup>.

## 1.4 Endothelial Cell Death Pathways

Transplantation is invariably associated with cell death, especially that of endothelial cells, which is the first barrier between cardiac grafts and the recipient's immune system<sup>64-66</sup>. During the transplantation process and especially ischemia, apoptosis and necroptosis are two pathways that can be initiated due to injury to the cells or because of pro-inflammatory factors<sup>66</sup>. Apoptosis can be triggered by death receptors such as tumor necrosis factor receptor or the mitochondrial outer membrane permeabilization (MOMP)<sup>56,66,67</sup>. Necroptosis is a form of caspase-independent cell death which can also be initiated by tumor necrosis factor alpha (TNF- $\alpha$ ) and occurs following caspase-8 inhibition<sup>66,68</sup>. Necroptosis is mediated by receptor interacting protein kinases 1 and 3 (RIPK1 and RIPK3)<sup>56</sup>. This form of cell death can lead to the release of inflammatory molecules such as HMGB1 and loss of membrane integrity<sup>66</sup>. Other forms of cell death such as ferroptosis and pyroptosis have been shown to impact endothelial cells in cardiac transplantations and cardiac-related pathologies but the pathways are not as well-defined as apoptosis and necroptosis<sup>69,70</sup>.

In solid organ transplantation, chronic graft rejection is a major obstacle in the long-term success of the transplant<sup>71</sup>. Growing evidence points to the important role of endothelial cells antibody-mediated acute rejection as well as chronic rejection<sup>72</sup>. During acute cellular rejection, endothelial cells are attacked by HLA I and II-recognizing immune cells, resulting in endothelial cell lysis after the complement system is activated<sup>73</sup>. Upon endothelial cell injury caused by environmental or innate stress post-transplantation, vascular lesions can occur<sup>71,74,75</sup>. These lesions can lead to thickening of the arterial intima, formation of fatty plaques, and ultimately heart failure<sup>74,75</sup>. One study which used heterotopic abdominal heart transplants found that cardiac myocytes, endothelial cells, and interstitial cells became apoptotic in the first five days following the transplantation procedure<sup>75</sup>. Interestingly, another study showed that in IRI, endothelial cell death preceded myocyte cell death in the heart<sup>76</sup>. During IRI, endothelial cell function is disrupted causing increased endothelial permeability because angiogenic growth factor

expression is increased and the release of proinflammatory mediators like cytokines and proteases<sup>40</sup>.

### 1.4.1 Apoptosis

Apoptosis was first described in 1972 and comprises the genetically determined elimination of cells<sup>67</sup>. It occurs in development and aging, as well as a homeostatic mechanism to maintain cell populations<sup>40,67</sup>. It can also be a defense or immune mechanism to remove damaged cells<sup>67</sup>. Cells expressing Fas or TNF receptors can bind ligands and cross-link proteins to lead to apoptosis<sup>66,67</sup>. The main characteristic feature of apoptosis is that of cell shrinkage and pyknosis with dense cytoplasm<sup>67</sup>. The chromatin condenses while the plasma membrane blebs, followed by karyorrhexis and the separation of cell fragments into apoptotic bodies during budding. Apoptotic bodies contain cytoplasm with packed organelles with or without a nuclear fragment and are then phagocytosed. The main pathways of apoptosis are the extrinsic or death receptor pathway, and the intrinsic or mitochondrial pathway<sup>66,67</sup>. These two pathways converge on the same execution pathway which is started by caspase-3 cleavage leading to DNA fragmentation, cytoskeletal and nuclear protein fragmentation, protein cross-linking, apoptotic body formation, and phagocytic cell uptake<sup>67</sup>. Apoptosis can be initiated by two different death triggers, either death receptors or MOMP<sup>56,66,67</sup>.

Intrinsic apoptosis can be controlled through intracellular signals caused by endogenous and exogenous stimuli such as ischemia or oxidative stress either by direct activation of caspase-3, by cleaving Bid (BH3 interacting domain death agonist), or other potential non-receptor-mediated stimuli<sup>67,77,78</sup>. When an injury occurs in the cell, p53, a sensor of cellular stress, will activate the pathway. It then activates pro-apoptotic proteins of the B-cell lymphoma 2 (Bcl-2) family, such as Bcl-2 associated x protein (Bax) or Bcl-2 homologous antagonist killer (Bak), causing a change in the inner mitochondrial membrane which leads to mitochondrial dysfunction<sup>67,77</sup>. This leads to MOMP, the opening of the MPTP and release pro-apoptotic molecules into the cytosol, such as second mitochondria-derived activator of caspase (SMAC)/direct inhibitor of apoptosis protein (IAP) binding protein with low pI (DIABLO) protein, cytochrome *c*, apoptosis-

inducing factor (AIF), endonuclease G, and caspase-activated DNase (CAD)<sup>67,79,80</sup>. Activation of caspase-9 and downstream caspases then occurs<sup>67,78</sup>.

Extrinsic apoptosis is controlled by transmembrane death receptors and is dependent on caspase-8 (Figure 3)<sup>67,77</sup>. The two initial receptors are either the first apoptosis signal receptor (Fas) or tumor necrosis factor receptor 1 (TNFR1). The binding of Fas ligand to Fas receptor recruits Fas-associated death domain protein (FADD) and pro-caspase-8 to form a death-inducing signalling complex (DISC). DISC then cleaves or activates caspase-8, triggering activation of caspase-3<sup>67</sup>. Caspase-3 then activates the endonuclease caspase-activated DNase (CAD) to cause double-stranded DNA breaks and DNA fragmentation<sup>67,81</sup>.

#### 1.4.2 Necroptosis

Necroptosis is a caspase-independent necrotic pathway, otherwise known as programmed or regulated necrosis<sup>34,40,56,66</sup>. It shares several features with accidental cell death, including organelle swelling, plasma membrane rupture, cell lysis, and leakage of intracellular components leading to secondary inflammatory responses<sup>66,82</sup>.

Necroptosis is regulated by receptor-interacting protein kinases 1 and 3 (RIPK1 and RIPK3), and downstream pseudokinase mixed-lineage kinase domain-like (MLKL) (Figures 3 and 4)<sup>56,68,77,83</sup>. It is induced by death receptors including Fas and TNFR1<sup>68,77</sup>. It can also be inhibited by necrostatin-1, a synthesized small molecule inhibitor of RIPK1<sup>56,68,83,84</sup>. Once TNFR1 is stimulated, the TNFR associated death domain (TRADD) is recruited to the plasma membrane. This recruits RIPK1, cellular inhibitors of apoptosis 1 and 2 (cIAP1 and cIAP2), linear ubiquitin chain assembly complex (LUBAC), and TNF receptor associated factor 2 and 5 (TRAF 2 and TRAF 5) to form complex I<sup>66,77</sup>. When RIPK1 is ubiquitinated due to cIAP 1, cIAP2, and LUBAC, nuclear factor- $\kappa$ B is activated to lead to cell survival. However, deubiquitylation of the K63 and linear ubiquitin chains of RIPK1 by enzymes A20 and cylindromatosis (CYLD) promotes cell death instead of survival as RIPK1 is dissociated from complex I<sup>66,77,85</sup>. RIPK1 then complexes with FADD, pro-caspase-8, and cellular FLICE-like inhibitory protein (c-FLIP) to form DISC or complex IIa. c-FLIP prevents caspase-8 activation and

processing, thus inhibiting apoptosis<sup>77</sup>. RIPK1 and RIPK3 interaction following deubiquitylation leads to the formation of the necrosome complex IIb through autophosphorylation and transphosphorylation<sup>66,68,77</sup>. RIPK1 and RIPK3 interact via intrinsic RIP homotypic-interacting motifs (RHIMs) to form a complex called the necrosome<sup>77,86-88</sup>. This complex then leads to the phosphorylation of MLKL via RIPK3, promoting MLKL oligomerization and movement into the plasma membrane<sup>66,77,86,89,90</sup>. This process results in membrane permeabilization and calcium efflux. The MLKL oligomer binding to the plasma membrane phosphatidylinositol phosphates leads to membrane pore openings and recruitment of ion channels, resulting in flux of ions such as calcium, sodium, and potassium<sup>68,77,86,88,89</sup>. This membrane permeabilization induces the release of cellular plasma material and danger-associated molecular patterns (DAMPs) that can promote inflammation. This DAMP-dependent systemic inflammation of feedback is referred to necroinflammation<sup>77,89</sup>. DAMPs include high-mobility group box 1 (HMGB1), cyclophilin A (CypA), and heat shock proteins<sup>89</sup>. Proinflammatory cytokines and chemokines may enter circulation due to inflammasome activation and cell lysis. Mitochondrial DNA can also be a cellular DAMP after release from the mitochondria<sup>77,89</sup>. This is measurable in systemic circulation in inflammatory diseases. Nuclear DNA degradation is a hallmark of cell death, and it has been well-documented that DNA degradation in apoptosis is mainly dependent on caspase activated DNAases<sup>67,91,92</sup>. However, the molecular mechanism for DNA degradation in necroptosis is not clear and requires further investigation.



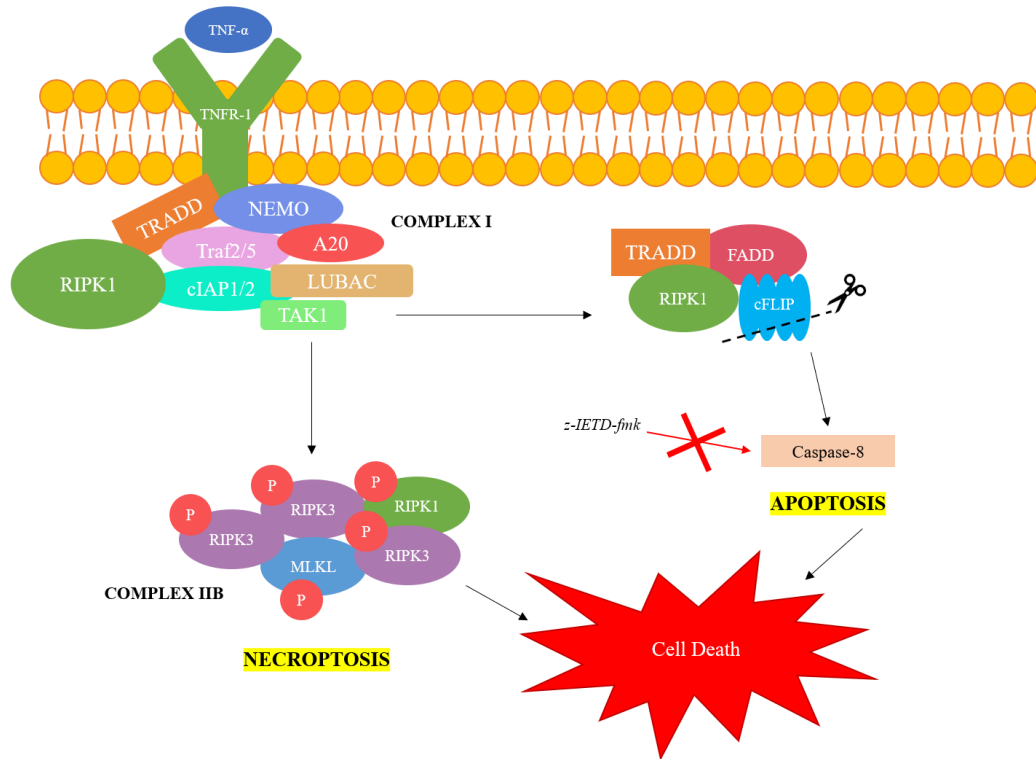


**Figure 3: Pathway of apoptosis vs. necroptosis**

In the context of ischemia-reperfusion injury, the major pathways of cell death include apoptosis and necroptosis<sup>66,93</sup>. The upstream pathway of extrinsic or death receptor-mediated apoptosis and necroptosis are shared, beginning with ligation of TNF- $\alpha$  with TNFR1<sup>66,77</sup>. This binding then recruits TRADD, cIAP1/2, LUBAC, TRAF2/5, and RIPK1 to the receptor to form complex I<sup>66,77</sup>. DISC is then formed with FADD, TRADD, RIPK1, and cFLIP in apoptosis<sup>94</sup>. cFLIP forms a complex with caspase-8 to suppress protease activity<sup>94</sup>. DISC results in the auto-catalytic activation of pro-caspase-8, leading to caspase-8 activation, triggering the execution phase of apoptosis<sup>67</sup>. When caspase-8 is inhibited, such as with caspase-8 inhibitor Z-Ile-Glu-Thr-Asp-Fluoromethylketone (z-IETD-fmk), complex Iib (necrosome) is formed instead with RIPK1, RIPK3, and MLKL<sup>68,77</sup>. This leads to necroptosis in the cell<sup>68,77,86</sup>. The mitochondria play an important role in these pathways especially in necroptosis as suggested by several studies<sup>77,85,95</sup>.

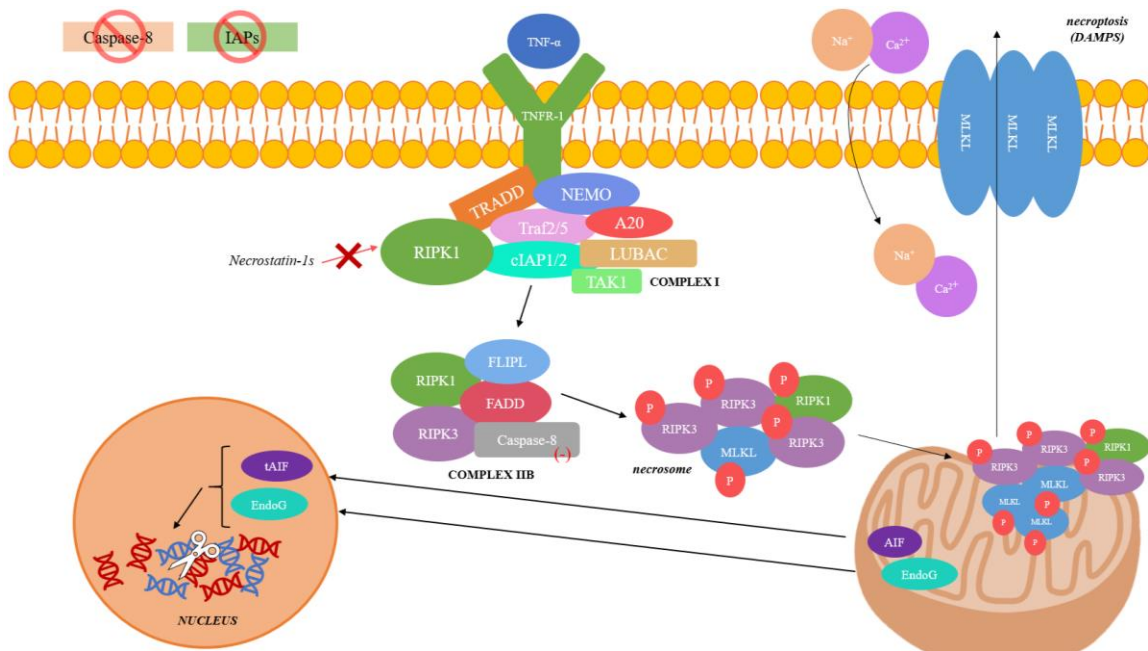


**Figure 4: Downstream pathway of necroptosis**

The most established pathway of necroptosis is initiated by the ligation of TNF- $\alpha$  to TNFR1<sup>77</sup>. This recruits TRADD, TRAF 2, TRAF 5, LUBAC, and RIPK1 to form complex I. RIPK1 can be ubiquitylated to lead to a pro-survival NF- $\kappa$ B pathway and can be inhibited with necrostatin-1 stable (nec-1s). The deubiquitylation of RIPK1 leads to the formation of complex IIa and then complex IIb after RIPK1 interacts with RIPK3<sup>77</sup>. The auto-phosphorylation and trans-phosphorylation of RIPK1 and RIPK3 then causes the phosphorylation of MLKL, initiating the downstream mechanisms of necroptosis<sup>77,85</sup>. The necrosome complex moves into the mitochondria where phosphorylated MLKL is oligomerized and translocates to the plasma membrane to cause membrane permeabilization, increase in calcium and sodium ion influx, and release of DAMPs which can promote distal tissue inflammation<sup>68,77,86,96</sup>. AIF and EndoG have been implicated in DNA degradation after translocation to the nucleus from the mitochondria<sup>97-99</sup>.

#### 1.4.2.1 Ferroptosis, Oxytosis, and Pyroptosis

Ferroptosis, oxytosis, and pyroptosis have been implicated in ischemia and IRI<sup>100-102</sup>. Ferroptosis is a regulated form of necrosis that uses iron-dependent lipid peroxidation to

function and can be inhibited by glutathione peroxidase 4<sup>85,86,102,103</sup>. It is characterized by lytic cell death, decreased mitochondrial membrane densities, reduction of the mitochondrial cristae, leading to mitochondrial membrane rupture<sup>85</sup>. Ferroptosis is induced by the compound erastin which inhibits the antiporter system X<sub>c</sub><sup>-</sup> by reducing glutathione levels<sup>85,103</sup>. System X<sub>c</sub><sup>-</sup> allows for the exchange of intracellular glutamine and extracellular cysteine exchange<sup>85,103</sup>. This leads to the accumulation of lipid peroxidation and an increase in iron mediated reactive oxygen species (ROS).

Oxytosis also involves the inhibition of system X<sub>c</sub><sup>-</sup>, where the production of ROS and the opening of cyclic GMP (cGMP)-gated channels lead to the influx of extracellular calcium ions<sup>85,104</sup>.

Pyroptosis is a lytic cell death form which is present in inflammatory and non-immune cells such as macrophages and endothelial cells respectively<sup>77</sup>. It can be triggered by bacteria, pathogens, and endotoxins. Following lysis, the membrane remains, helping to trap pathogens using pore-induced intracellular traps, release of DAMPs, and the movement of neutrophils to limit local inflammation<sup>77</sup>.

#### 1.4.2.2 Parthanatos

Parthanatos is another regulated form of necrosis that involves the overexpression of a nuclear protein poly adenosine diphosphate-ribose (ADP-ribose) polymerase 1 or PARP-1, which attaches a negatively charged polymer poly (ADP-ribose) (PAR) to itself<sup>85,105,106</sup>. Under normal physiological conditions, PARP-1 detects DNA damage leading to the synthesis of PAR chains and mediates the repair of various types of DNA damage including single-strand breaks, double-stranded breaks, and chromatin modification<sup>105-107</sup>. However, when there is excessive DNA damage, PARP-1 becomes overactivated<sup>107-109</sup>. This has also been shown to occur during IRI<sup>110</sup>. This activated PARP transfers ADP-ribose from nicotinamide adenine dinucleotide (NAD<sup>+</sup>), a co-factor in glycolysis and the citric acid cycle, to targets including apoptosis-inducing factor (AIF)<sup>108,109</sup>. Translocation of AIF from the mitochondria into the nucleus facilitates large-scale (50 kilobases) DNA fragmentation and cell death<sup>105,111</sup>. The NAD<sup>+</sup> overconsumption leads to NAD<sup>+</sup> depletion which impacts ATP generation causing cell

death, namely parthanotos<sup>108,112</sup>. Downstream of AIF, the nuclease macrophage migration inhibitor factor (MIF) was shown to be involved in large-scale DNA fragmentation in parthanatos<sup>113</sup>.

## 1.5 Mitochondrial Permeability Transition Pore

The mitochondrial permeability transition pore (MPTP) is important in cell death pathways and is located in the inner mitochondrial membrane<sup>42,51,112</sup>. When the MPTP opens, the inner membrane becomes non-selectively permeable to low molecular weight molecules below 1.5 kDa<sup>114,115</sup>. Following pore openings, the mitochondria become depolarized which triggers mitochondrial swelling due to increased osmotic pressure<sup>112,114,115</sup>. Various molecules are released from the mitochondria, which are not limited to calcium ions and pro-apoptotic molecules from the intermembrane space such as cytochrome *c*<sup>112,115</sup>. In ischemia-reperfusion injury, the mitochondria are depolarized during ischemia due to anaerobic metabolism<sup>47</sup>. The MPTP is inhibited during ischemia due to low pH but is opened once reperfusion raises the intracellular pH to 7 and above<sup>47</sup>.

## 1.6 Apoptosis-Inducing Factor

Mitochondrial molecules may contribute to DNA damage and impact cell death pathways<sup>110,116–118</sup>. The mitochondrial apoptosis-inducing factor (AIF) is a protein with NADH oxidase activity located in the inner mitochondrial membrane<sup>110,111,116,119–121</sup>. It can be considered an oxidoreductase in the mitochondria and has a pro-apoptotic function in the nucleus<sup>110,111,116,119–121</sup>. In the nucleus, AIF is synthesized from a nuclear gene as a precursor form of 67 kDa<sup>116,122,123</sup>. It is then translocated to the mitochondria and processed via proteolytic cleavage to a mature form of 62 kDa<sup>116,122</sup>. In this configuration, AIF becomes an inner membrane-anchored protein, with a N-terminal exposed to the mitochondrial matrix and a C-terminal exposed to the intermembrane space<sup>111,116,122</sup>. The C-terminal of AIF encloses its pro-apoptotic function, with five anti-parallel  $\beta$ -strands, two  $\alpha$ -helices, and a large loop<sup>121</sup>. AIF plays a role in the respiratory chain stability and maintenance of the mitochondrial structure<sup>116,121</sup>. AIF can be cleaved by cysteine proteases such as calpains and cathepsins to yield soluble tAIF (57 kDa), an apoptogenic protein<sup>80,116,122,124,125</sup>. It is then released from the mitochondria to the cytosol

following permeabilization of the outer mitochondrial membrane<sup>120,122</sup>. This is done by proteins such as Bax which regulate tAIF through outer mitochondrial membrane pores<sup>116,126</sup>. tAIF then interacts with different targets in the cytosol<sup>116</sup>. In PCD, tAIF translocates to the nucleus<sup>127</sup>. This translocation from the cytoplasm into the nucleus is positively regulated by CypA and negatively regulated by heat shock protein 70 (Hsp70)<sup>116,122,124,127,128</sup>. PARP-1 has also been shown to mediate release of AIF, a downstream molecule in parthanatos, in a caspase-independent manner<sup>110,119,122,127</sup>. AIF has also been shown to be involved in caspase-independent necroptosis<sup>97,98</sup>. Once in the nucleus, the truncated form of AIF associates with phosphorylated histone H2AX ( $\gamma$ H2AX) and CypA to provoke caspase-independent chromatin condensation, DNA degradation, and cell death<sup>91,116,119,122,125,127</sup>. The DNA degradation was shown to be in 20-50 kb fragments<sup>124</sup>. This nuclear translocation and induction of DNA damage has been shown to occur in response to pathologies including ischemia and cancer<sup>123,129</sup>. AIF does not have intrinsic endonuclease activity, so AIF-mediated DNA degradation depends on downstream nucleases<sup>124</sup>. There has been research suggesting cooperation between AIF and EndoG, released in a caspase-independent manner<sup>116,124</sup>. There is also the nuclease macrophage migration inhibitor factor (MIF) which is implicated in parthanatos<sup>113</sup>.

AIF is a promising target in addressing end-stage mechanisms in cell death such as nuclear fragmentation which are relevant to transplant rejection and allograft rejection<sup>131</sup>. A previous study in our lab found that cyclophilin D (CypD), an important molecule in formation of MPTP, may regulate the nuclear translocation of AIF<sup>132</sup>.

## 1.7 Study Rationale

Extended ischemic time during cardiac transplant has been associated with worse outcomes<sup>11,38,39</sup>. IRI leads to a decrease in intracellular and extracellular pH due to the change to anaerobic metabolism in ischemia<sup>33,34,46</sup>. Many clinical trials have failed to prevent IRI and there is currently no treatment which completely prevents IRI<sup>133</sup>.

Understanding the mechanism of cell death under low pH condition will help to develop specific treatment. In this project, we aimed to determine the role that AIF may have in ischemia by mimicking the acidic conditions that occur during ischemia.

## 1.8 Hypothesis

In an acidic extracellular environment, cell death patterns will be altered, and apoptosis-inducing factor will translocate into the nucleus to facilitate nuclear fragmentation.

## 1.9 Study Aims

- (1) To investigate the translocation of AIF from the mitochondria to the nucleus in necroptosis induction at physiological pH conditions and at acidic conditions.
- (2) To demonstrate DNA fragmentation in the nucleus following AIF translocation,
- (3) To study the role of PARP-1 in AIF translocation and DNA damage at acidic and physiological pH conditions,
- (4) To identify the nuclease which participates in AIF mediated-DNA damage.

## Chapter 2

### 2 Materials and Methods

#### 2.1 Mice

Wild-type (WT) male inbred C57BL/6 (B6) mice were purchased from the Jackson Laboratory (Bar Harbor, ME, USA). The mice were maintained in the Animal Care and Veterinary Services facility at Western University. The animal use protocol (AUP 2019-131) and experimental procedures were approved by the institutional Animal Care Committee.

#### 2.2 Endothelial Cell Culture

Murine MVECs were isolated as previously described and previously harvested frozen cell cultures were used<sup>131</sup>. WT B6 male inbred mice were euthanized with carbon dioxide. Heart ventricles were collected from 3 weeks old wild-type B6 mice and minced to remove the blood cells after being washed in phosphate buffer. Aortic tissue and atria were removed. Minced hearts were then incubated in a digestion buffer with collagenase II (1 mg/mL; Sigma-Aldrich) at 37°C for 40 minutes. Debris were removed with a 100 µm nylon mesh filter (Thermo Scientific). Cell suspension was then incubated with anti-CD31 coated Dynabeads™ M450 beads (Thermo Scientific) for 30 minutes and then washed in a magnet block (MACS, Miltenyi Biotec) three times. CD31-positive cells were then grown in complete Endothelial Cell Basal Medium-2 (EBM-2; Lonza) supplemented with 5% fetal bovine serum (FBS), 0.04% hydrocortisone, 0.04% hBFB-b, 0.1% VEGF, 0.1% R3-IFG-1, 0.1% ascorbic acid, 0.1% hEGF, and 0.1% GA-1000 (Lonza). MVECs were immortalized through transfection of origin-defective SV40 DNA using the calcium-phosphate co-precipitation method (Invitrogen)<sup>131</sup>. MVEC phenotype was confirmed using flow cytometry confirming the presence of CD31, CD102, and CD105<sup>131</sup>. The percent positivity of CD31, CD102, and CD105 were 69.8%, 86.9%, and 80.3% respectively.

Normal cell culture medium used to grow the endothelial cells was prepared by supplementing 1 g/L glucose Dulbecco's Modified Eagle Medium (DMEM; Gibco) with

10% FBS and 1% penicillin/streptomycin. The phenotype of MVECs was re-confirmed with flow cytometry following the switch from EBM-2 to DMEM. Cells were kept in a humidified incubator (37°C; 5% CO<sub>2</sub>).

The MVECs were initially thawed from frozen vials originating from the same culture and passage. To passage, adherent cells were washed with 1x Dulbecco's phosphate-buffered saline (DPBS) before being dissociated from plastic with 0.25% trypsin (Gibco). Cells were passaged a maximum of ten times before being discarded.

## 2.3 Cell Death Assay

### 2.3.1 pH Adjustment of Cell Media

Culture medium, DMEM (Gibco), in a powder form with low glucose (1000 mg/mL) and glutamine but lacking sodium bicarbonate and serum was re-constituted using tissue culture grade water. The media was warmed in the incubator for one hour to reach a temperature of 37°C before the pH was measured using a pH meter (Hach Company). Following this, the media was adjusted using hydrochloric acid to pH 6.5 to be used in the cell death assays to stimulate the acidic conditions that occur during ischemia. Ischemic rat hearts were shown to have measurements of pH between 5.5 to 6.8, while another publication stated that the intracellular and extracellular pH during ischemia could fall as low as 6.0 to 6.5<sup>8,134,135</sup>. In addition, it has been reported that the pH in ischemic solid tissues can fall by one or more logarithmic units of pH<sup>112</sup>. A pH of 6.5 was selected because ischemic times are limited as much as possible for cardiac transplantations, suggesting that the measured change in pH would be on the lower side of the spectrum<sup>11,37-39</sup>. Cell culture medium measured at pH 7.4 was used as a comparison of normal physiological conditions.

### 2.3.2 Real-Time Cell Death via IncuCyte

Cell death was detected and quantified through real-time imaging using the IncuCyte ZOOM® Live Cell Analysis System (Sartorius). SYTOX™ Green Nucleic Acid Stain (Invitrogen) at 100 nM to indicate cell death as it crosses the permeabilized plasma membranes of dead cells, staining the nucleic acid. It is excited at 440-480 nm in the



IncuCyte and green fluorescence is captured at 504-544 nm, to help distinguish dead cells with positive SYTOX™ Green Nucleic Acid Stain from live cells. Cells were cultured to a ~70% confluent monolayer in clear 96-well plates ( $4 \times 10^3$  cells/well) and treated with the following reagents. Human TNF- $\alpha$  (hTNF- $\alpha$ , 20ng/well, PeproTech) [T] was used to induce cell death. SMAC mimetic (BV6, 0.1  $\mu$ M, APEX-BIO) [S] was added to prevent the function of inhibitor of apoptosis proteins (IAPs), causing caspase activation and leading to apoptotic cell death<sup>136,137</sup>. Apoptosis was blocked using caspase-8 inhibitor Z-Ile-Glu-Thr-Asp-Fluoromethylketone (IETD, 30  $\mu$ M, APEX-BIO) [I]<sup>138</sup>. RIPK1 inhibitor necrostatin-1 stable (Nec-1s, 10  $\mu$ M, BioVision) [N] was added to inhibit necroptosis<sup>84</sup>. The CypA inhibitor, Alisporivir (DebioPharm) was used at 0.25-50  $\mu$ M to prevent AIF translocation<sup>139,140</sup>. The PARP-1 inhibitor, 3 aminobenzamide (3-ABA, Sigma-Aldrich) was used at 1-200  $\mu$ M to inhibit parthanatos<sup>99</sup>. Using dose response curves to see the inhibitory effects of Alisporivir and 3-ABA on cell death at pH 7.4 and 6.5, 4  $\mu$ M of Alisporivir and 100  $\mu$ M of 3-ABA were selected for this project. As a positive control, 0.1% Triton™ X-100 (TX100), a non-ionic surfactant, was used to induce 100% cell death by permeabilizing cellular and nuclear membranes. This was then used to calculate the percentages of cell death in all treatment groups.

### 2.3.3 Cell Death and Apoptosis Quantification with Flow Cytometry

Cell death was also confirmed using propidium iodide (PI) and annexin V labelling. Cells were grown to a ~70% confluent monolayer in a 12-well plate ( $10^5$  cells/well) and treated with the previously listed concentrations of TNF- $\alpha$ , SMAC, IETD, necrostatin-1s for the following treatment groups: untreated [UT], TS, TSI, TSN, TSIN. Following a 12-hour death assay, the spent media culture was collected in round-bottom polystyrene test tubes labelled for each treatment. The cells were washed with DPBS before 0.25% trypsin was added to the wells to dissociate the cells from the plates. The reaction was stopped with DMEM supplemented with 10% FBS and the liquid was added to the test tubes. The tubes were then centrifuged for 5 minutes at 500 g and the pellets were resuspended in annexin V-PI binding buffer. Stains for annexin V (BD Pharmingen) and propidium iodide (BD Pharmingen) were added to the tubes and incubated in the dark for 15 minutes before additional annexin V binding buffer was added to the cell suspension.

Samples were then run on a 4-laser CytoFLEX S flow cytometer (Beckman Coulter) with the following laser gains for the respective channels: 50 FSC, 50 SSC, 20 FITC (for annexin V), 10 PerCP (for propidium iodide). Unstained healthy cells, cells stained with annexin V only, and cells stained with PI only were used for compensation. Experiments were repeated at least three times.

## 2.4 Immunocytochemistry

To visualize AIF translocation from the mitochondria into the nucleus of endothelial cells undergoing apoptosis and necroptosis, endothelial cell cultures in 96-well plates coated with poly-D-lysine (Gibco) were subjected to the cell death assays described earlier. The timepoint where cell death began to sharply increase in the various treatment groups was used as the endpoint. At this timepoint, the cells were washed with DPBS and fixed with 4% paraformaldehyde (Thermo Scientific) in DPBS at pH 7.4 for 30 minutes at room temperature. The cells were then washed for five minutes thrice with DPBS-T (DPBS with 0.1% Tween-20) before being incubated with 0.25% TX100, in DPBS at room temperature for 10 minutes to permeabilize all lipid membranes. Cells were washed thrice for five minutes again with DPBS-T (used for all subsequent washes) before being incubated in a blocking solution (3% bovine serum albumin (BSA), 22.52 mg/mL glycine, 0.1% Tween-20, 10% normal goat serum) for one hour at room temperature to decrease non-specific antigen binding and background fluorescence. Following this, the cells were incubated with primary rabbit anti-mouse AIF antibody (Abcam) diluted in 1% BSA in DPBS with 0.1% Tween-20 at a concentration of 1:1000 overnight at 4°C. The following day, the cells were washed again 3x for 5 minutes each with DPBS and then incubated with a secondary biotinylated goat anti-rabbit IgG antibody (H+L) (Vector Laboratories) diluted at 1:500 in 1% BSA in DPBS with 0.1% Tween-20 for one hour. Afterwards, the secondary antibody was removed, and the cells were incubated with PE-conjugated streptavidin (eBioscience) for one hour. The cells were washed 3x for 5 minutes with DPBS-T and the nuclei were then counterstained with 150 nM DAPI dilactate (Invitrogen) in DBPS for five minutes. The cells were washed 3x for 5 minutes with DPBS-T before adding in fresh DPBS to the wells. Cells were then imaged using an Inverted Research Microscope ECLIPSE Ts2R (Nikon) at 20x and 40x magnification.

In order to see whether or not endonuclease G (EndoG) participates with AIF to cause nuclear fragmentation, the same protocol for immunocytochemistry staining was performed as indicated above. The primary antibody was anti-mouse EndoG (Santa Cruz Biotechnology) diluted at 1:500 in 1% BSA in DPBS with 0.1% Tween-20 and incubated overnight at 4°C. The secondary antibody was a biotinylated goat anti-mouse IgG antibody (H+L) (Chemicon, Sigma-Aldrich) diluted at 1:250 in 1% BSA in DPBS with 0.1% Tween-20 and incubated for one hour.

#### 2.4.1 Quantification of Positive Nuclear Translocation

Images of AIF or EndoG red immunofluorescence or nuclear blue fluorescence were taken of the cells following immunocytochemistry and were then quantified for positive nuclear translocation of AIF or EndoG following the death assay. Cells used for repeated experiments came from frozen cell cultures which initially originated from the same flask. In each experiment, there were at least three replicate wells per treatment on the 96-well plates used at pH 7.4 and 6.5, so at least one photo was taken of each well at 20x magnification. The overall experiment was repeated three times at each pH. Total number of cells and total positive cells were manually counted by two individuals blinded to the treatment and the percentage of positive nuclear translocation was averaged between the two counts per image.

## 2.5 RNA Interference Silencing

Wild-type endothelial cells were seeded onto 6-well plates at 60-80% confluency ( $100-150 \times 10^3$  cells/well). The cells were washed with DPBS twice before transfection of *Aifm1* siRNA (Dharmacon) using EndoFectin™ Max transfection reagent in Opti-MEM™ media. The pre-designed target sequence was GAGUAGAGCAUCAUGAUCA. A dose-response from 5-200 nM of the mouse *Aifm1* siRNA was performed to determine the optimal concentration of siRNA. Based on the data from RT-qPCR, a concentration of 50 nM was selected for the study. The AIF-silenced cells were collected from the plate with 0.25% trypsin after a 24-hour transfection before being plated on 96-well plates to run cell death assays as described earlier. Endothelial cells with only EndoFectin™ Max

transfection reagent in Opti-MEM™ media were used as a control for RT-qPCR and for the cell death assays following silencing.

## 2.6 RT-qPCR

siRNA-induced silencing of *Aifm1* expression was confirmed using RT-qPCR at 24 hours post-transfection. Total RNA from *Aifm1* siRNA transfected and control cells were extracted using the Qiagen RNeasy Mini Kit following the manufacturer's protocol. The concentration and purity of the isolated RNA was measured using the GENESYS™ 10S UV-Visible spectrophotometer (Thermo Scientific) and 500ng of RNA was used for cDNA synthesis. cDNA was generated from the RNA using the OneScript® Plus cDNA Synthesis Kit (ABM). RT-qPCR was run using the PowerTrack™ SYBR Green Master Mix (Applied Biosystems) on the CFX Connect™ Real-Time PCR Detection System (Bio-Rad). The *Aifm1* primers used were as follows: *Aifm1* forward primer (5' – 3') GTA GAT CAG GTT GGC CAG AAA CTC and *Aifm1* reverse primer (3' – 5') GGA TTA AAG GCA TGT GCC AAC ACG.  $\beta$ -actin was used as an internal control for gene expression and the primers were as follows:  $\beta$ -actin forward primer (5' – 3') CCA GCC TTC CTT CCT GGG TA and  $\beta$ -actin reverse primer (3' – 5') CTA GAA CAT TTG CGG TGC A. The  $\Delta$ Ct values for *Aifm1* and  $\beta$ -actin were used to calculate the  $2^{-\Delta\Delta C_t}$  for expression fold change.

## 2.7 Western Blots

siRNA-induced silencing of *Aifm1* was also confirmed with western blot analysis at 24 hours post-transfection. Total protein from control (EndoFectin™ Max transfection reagent only in Opti-MEM™ media) and *Aifm1* siRNA-transfected (50 nM of siRNA and EndoFectin™ Max transfection reagent in Opti-MEM™ media) cells were extracted using RIPA Lysis Buffer System (Santa Cruz Biotechnology). The concentration and purity of the protein was measured against a BSA standard curve using the Pierce™ BCA Protein Assay Kit (Thermo Scientific) following the manufacturer's protocol. Absorbance values were measured on the iMark™ Microplate Absorbance Reader at a wavelength of 570 nm. The isolated protein samples were then denatured by boiling in a loading buffer (4% SDS, 5%  $\beta$ -mercaptoethanol, 20% glycerol, 0.0004% bromophenol

blue, 0.125 M Tris-HCl; pH adjusted to 6.8) at 95°C for 5 minutes. The protein samples were then equally loaded (40 µg/well) into the wells of an SDS-PAGE gel made of a 4% acrylamide stacking gel and 12% acrylamide resolving gel. The gel was run at 60V through the stacking gel and 100V for the resolving gel in the electrophoresis system with a 1x running buffer (25 mM Tris base, 192 mM glycine, 0.1% SDS; pH adjusted to 8.3). The separated protein samples were transferred onto a polyvinylidene fluoride (PVDF) membrane activated with methanol in transfer buffer (25 mM Tris-HCl, 192 mM glycine, 20% v/v methanol; pH adjusted to 8.3) using a wet-tank transfer system. The transfer cassette was made with a PVDF membrane, filter paper, fiber pads, and the SDS gel surrounded by ice and run at 90V for 70 minutes. After the proteins were transferred onto the PVDF membrane, the transfer membrane was blocked with 5% low-fat skim milk in TBS-T (20 mM Tris base, 150 mM NaCl, 0.1% Tween-20), except in the case of phosphorylated RIPK1 (p-RIPK1), where 3% BSA dissolved in TBS-T was used instead, on a shaker for 1 hour at room temperature. The PVDF membrane was then incubated with primary rabbit anti-mouse AIF monoclonal antibody (Cell Signaling Technology) diluted 1:1000 in 2.5% non-fat dry milk in TBS-T overnight at 4°C. The PVDF membrane was then washed three times for 15 minutes with TBS-T before being incubated with secondary goat anti-rabbit IgG HRP-linked antibody (Cell Signaling Technology) diluted 1:1000 in 2.5% non-fat dry milk in TBS-T overnight at 4°C. The membrane was washed 3x for 10 minutes with TBS-T before it was incubated with Immobilon Western Chemiluminescent HRP Substrate (Millipore) for 5 minutes at room temperature. The PVDF membrane was then imaged on the FluorChem M Imaging System (ProteinSimple). The housekeeping gene GAPDH (Santa Cruz Biotechnology) was used as a loading control and densitometry analysis was performed with the software package AlphaView (ProteinSimple).

In addition to confirming siRNA-induced silencing of the *Aifm1* gene, western blots were also run to determine total RIPK1 and phosphorylated RIPK1 protein expression following a death assay as described above. Cells were treated at pH 7.4 and 6.5 for 3 hours before being lysed with the RIPA Lysis Buffer System (Santa Cruz Biotechnology) as described above. The primary antibodies were rabbit anti-mouse polyclonal phospho-RIPK1 (Ser166) (Invitrogen) and rabbit anti-mouse monoclonal RIPK1 (Abcam) were

diluted 1:1000 and the secondary antibody was a goat anti-rabbit IgG HRP-linked antibody (Cell Signalling Technology). GAPDH (Santa Cruz Biotechnology) was used as a loading control.

## 2.8 DNA Gel Analysis

To analyze AIF-mediated degradation of DNA, endothelial cells were cultured on 6-well plates to about 70% confluency and treated as described in section 2.3.2 for up to 45 hours at pH 6.5 and 7.4. The supernatants were collected and centrifuged to collect any floating or dead cells. The adherent cells were combined with pelleted cells before being lysed overnight at 56°C with 0.5 mg/mL proteinase K dissolved in a cell lysis buffer (50 nM NaCl, 5 mM EDTA, 5 mM Tris at pH 8, 20 mM DTT, 1% SDS). The lysates were centrifuged at  $1600 \times g$  room temperature to pellet cell debris and supernatants were transferred to fresh tubes for phenol-chloroform extraction. An equal volume of phenol:chloroform:isoamyl alcohol (25:24:1) was added to the samples and vortexed for one minute to mix. Samples were then centrifuged at  $1600 \times g$  for 5 minutes, and the upper aqueous layer was moved into clean tubes. Ethanol precipitation was conducted by adding 1  $\mu$ L of 20 mg/mL glycogen, 0.5 x sample volume of 7.5 M  $\text{NH}_4\text{OAc}$ , and 2.5 x sample volume of 100% ethanol to the aqueous samples. The samples were placed at -20°C overnight to precipitate the DNA, centrifuged for 10 minutes at  $1600 \times g$  at 4°C to form a DNA pellet which then underwent two 70% ethanol washes before being air dried and dissolved in 1x TE buffer. DNA was quantified using the DS-11 DNA Quantification Spectrophotometer (DeNovix). In a 1% agarose gel, 500 ng of DNA was loaded per lane. For DNA visualisation, the agarose gel was stained with SYBR<sup>TM</sup> Safe DNA gel stain and imaged on the ProteinSimple FluorChem M Imaging System.

## 2.9 Statistical Analysis

Statistical analysis was completed using GraphPad Prism 8. The data is represented as the mean  $\pm$  SD with at least 3 independent measurements or biological replicates in an experiment. Each experiment was repeated at least 3 times. Data was analyzed using Student's t-test for paired values and 1- and 2-way analysis of variance (ANOVA) with

Tukey's post-hoc corrections test. Differences were considered statistically significant when the p-value  $\leq 0.05$ .

## Chapter 3

### 3 Results

#### 3.1 Acidic pH Inhibits TNF- $\alpha$ -Mediated Necroptosis in Endothelial Cells

Wild type microvascular endothelial cells were used to determine the impact of pH on cell death. TNF- $\alpha$ , SMAC-mimetic BV6, caspase-8 inhibitor z-IETD-fmk, or RIPK1 inhibitor necrostatin-1s were added to the wild type B6 MVEC cultures using media that was adjusted to either 7.4 or 6.5. In the pH 7.4 treatments, the addition of TNF- $\alpha$  and BV6 increased cell death compared to untreated (UT) cells (Figure 5). Adding z-IETD-fmk also increased cell death more than untreated cells, suggesting necroptotic cell death. Necroptosis was inhibited with RIPK1 inhibitor necrostatin-1s, lowering cell death levels almost to baseline in the TNF- $\alpha$  + BV6 + z-IETD-fmk + necrostatin-1s group.

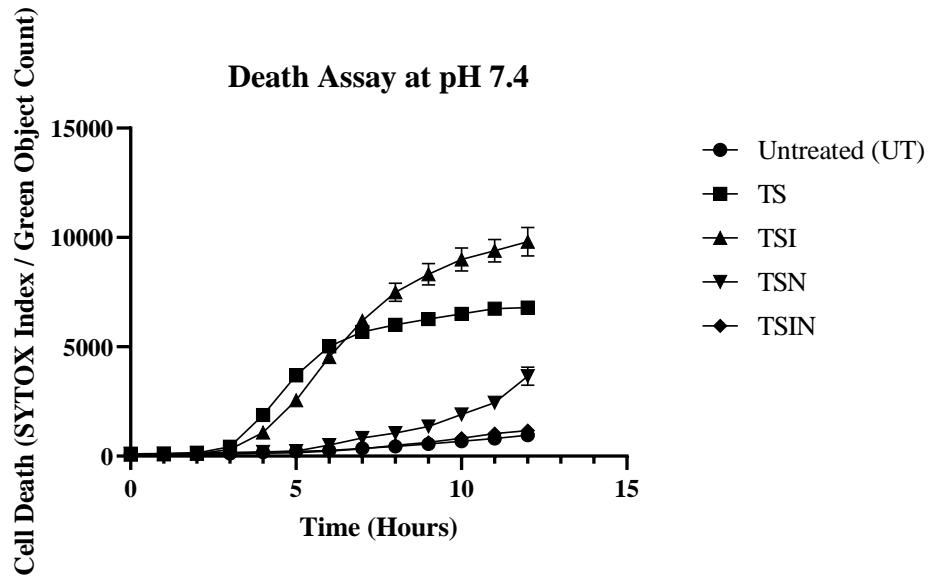
However, changes to cell death levels were seen in the pH 6.5 treatments. While the addition of TNF- $\alpha$  and BV6 increased cell death compared to untreated cells, the combination of TNF- $\alpha$ , BV6, and z-IETD-fmk showed an inhibition of cell death as measured by the Incucyte Image system (Figure 6). Hence, our data showed that low pH conditions altered necroptotic cell death to an apoptosis-like cell death.

While the Incucyte detects cell death via nuclear uptake of SYTOX Green, flow cytometry was used as a second method to confirm the cell death modality by detecting annexin V and propidium iodide positive cells for treatments at pH 6.5 (Figure 7).

Annexin V detects phosphatidylserine, a cell membrane component which translocates from the inner to outer membrane leaflets during apoptosis, exposing itself to the external environment of the cells. Propidium iodide binds double stranded DNA in cells when both cell and nuclear membranes become permeable. The death assays on the Incucyte also showed that the rate of cell death reached its peak at around the 12-hour mark for MVECs at both pH 7.4 and 6.5. Thus, the immunocytochemistry experiments which examined AIF translocation were performed 12 hours after the start of the death assays.



A



B

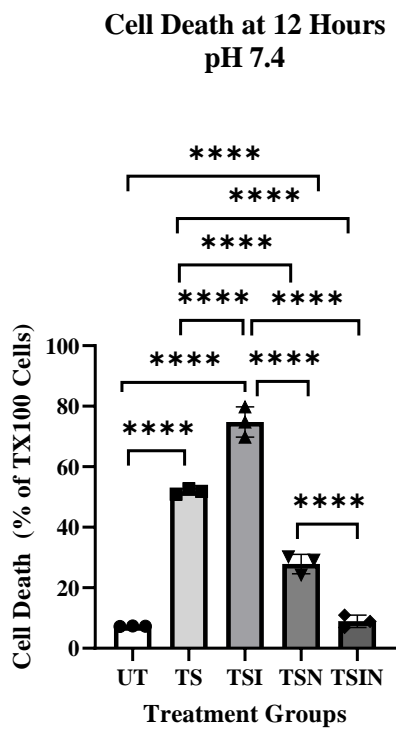
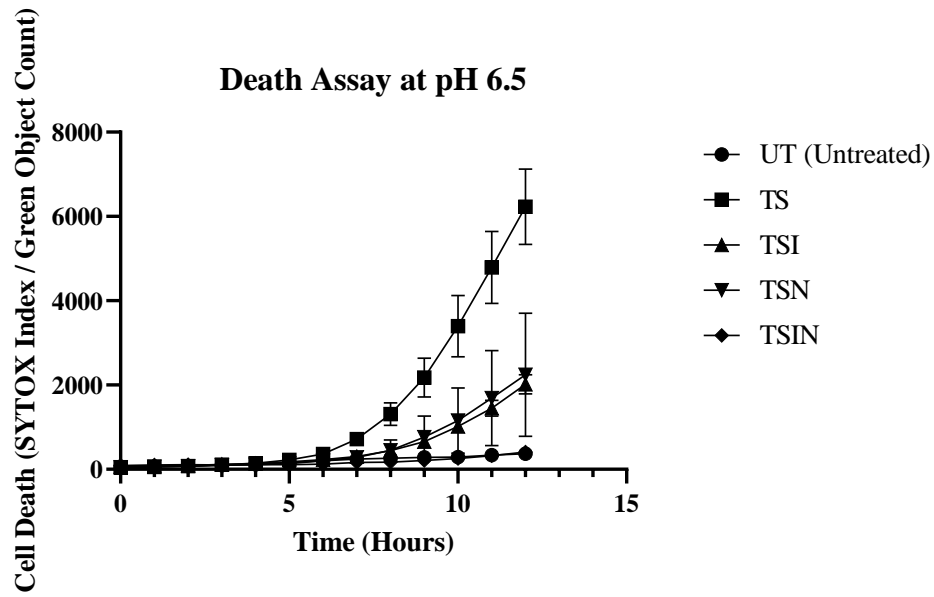


**Figure 5: Apoptosis and necroptosis in endothelial cells at pH 7.4**

- (A)** WT B6 endothelial cells were cultured in a 96-well plate in triplicate to ~70% confluency. Complete cell culture media was replaced with medium lacking antibiotics and serum at physiological pH of 7.4. hTNF- $\alpha$  at 20ng/well [T], SMAC mimetic at 0.1  $\mu$ M [S], IETD at 30  $\mu$ M [I], and Nec-1s at 10  $\mu$ M [N] were added to simulate the ischemic environment. SYTOX™ Green Nucleic Acid Stain at 100 nM was used as a nuclear stain to indicate dead cells. Cell death was detected and quantified using the IncuCyte ZOOM® Live Cell Analysis System. For positive control (not shown), 0.1% Triton™ X-100 (TX100), a non-ionic surfactant was used to induce 100% cell death and to calculate the percent of cell death in all treatments.
- (B)** Data at 12 hours from the start of the death assay are shown as mean  $\pm$  SD and representative of at least 3 independent experiments; n=3; \*\*\*\*p $\leq$ 0.0001, ns = non-significant (p-value  $\geq$  0.05); 1-way ANOVA; Tukey's multiple comparisons test.

A



B

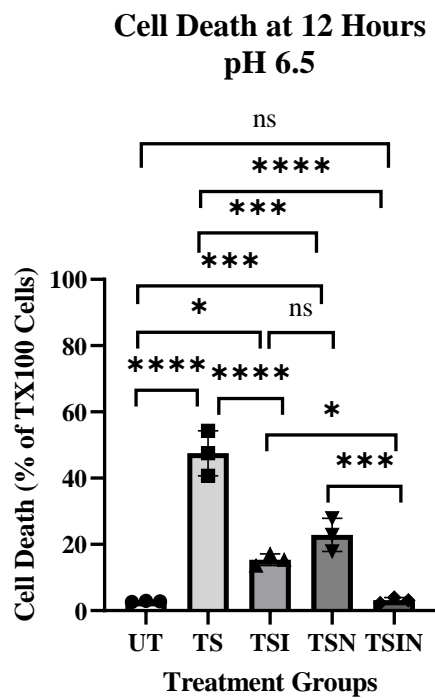
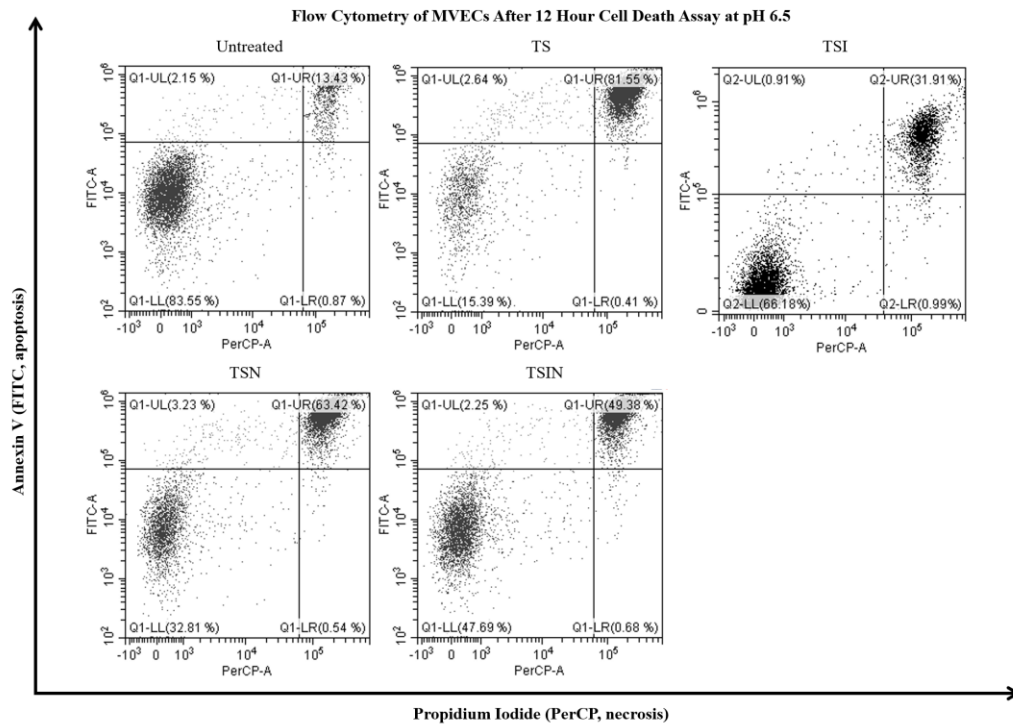


**Figure 6: Inhibition of necroptosis in endothelial cells at pH 6.5**

- (A)** WT B6 endothelial cells were cultured in a 96-well plate in triplicate to ~70% confluency. To model acidosis which occurs in ischemia, complete cell culture was replaced with prepared culture medium adjusted to pH 6.5. hTNF- $\alpha$  at 20ng/well [T], SMAC mimetic at 0.1  $\mu$ M [S], IETD at 30  $\mu$ M [I], and Nec-1s at 10  $\mu$ M [N] were added to stimulate an ischemic environment. SYTOX<sup>TM</sup> Green Nucleic Acid Stain at 100 nM was used as a nuclear counterstain to indicate dead cells. Cell death was detected and quantified using the IncuCyte ZOOM<sup>®</sup> Live Cell Analysis System. For positive control (not shown), 0.1% Triton<sup>TM</sup> X-100 (TX100) was used to induce 100% cell death and to calculate the percent of cell death in all treatments.
- (B)** Data at 12 hours from the start of the death assay are shown as mean  $\pm$  SD and representative of at least 3 independent experiments; n=3; \*\*\*\*p $\leq$ 0.0001, \*\*\*p $\leq$ 0.0002, \*\*p $\leq$ 0.0021, \*p $\leq$ 0.0332, ns = non-significant (p-value  $\geq$  0.05); 1-way ANOVA; Tukey's multiple comparisons test.

A



B

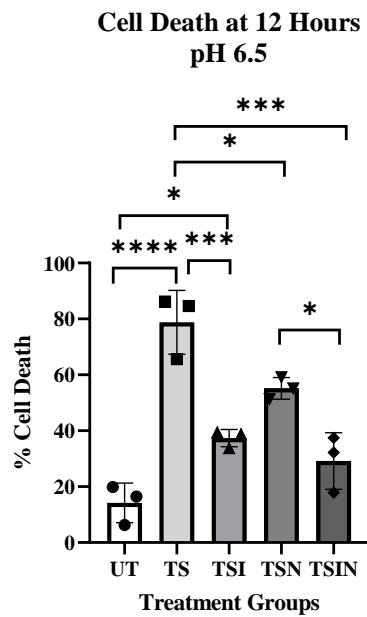


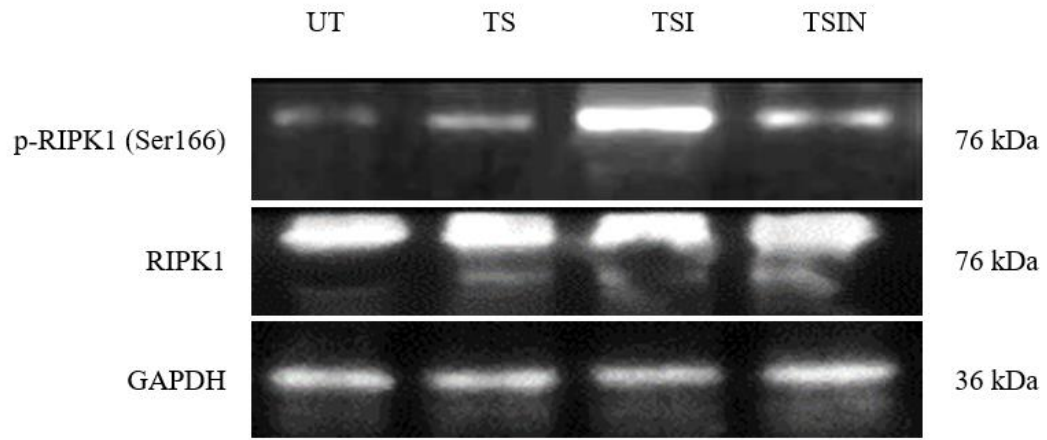
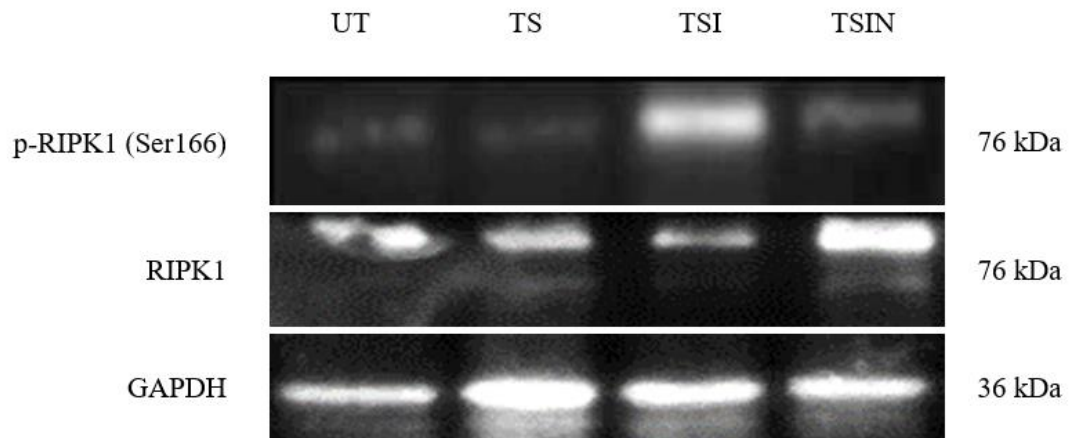
**Figure 7: Cell death at pH 6.5 mainly leads to apoptosis in endothelial cells**

Flow cytometry results using Annexin V and propidium iodide staining. MVEC's were subjected to the cell death assay as previously mentioned at pH 6.5 for 12 hours. Results were quantified for cell death. The cell death modality was mainly apoptosis based on the Annexin V and propidium iodide staining results.

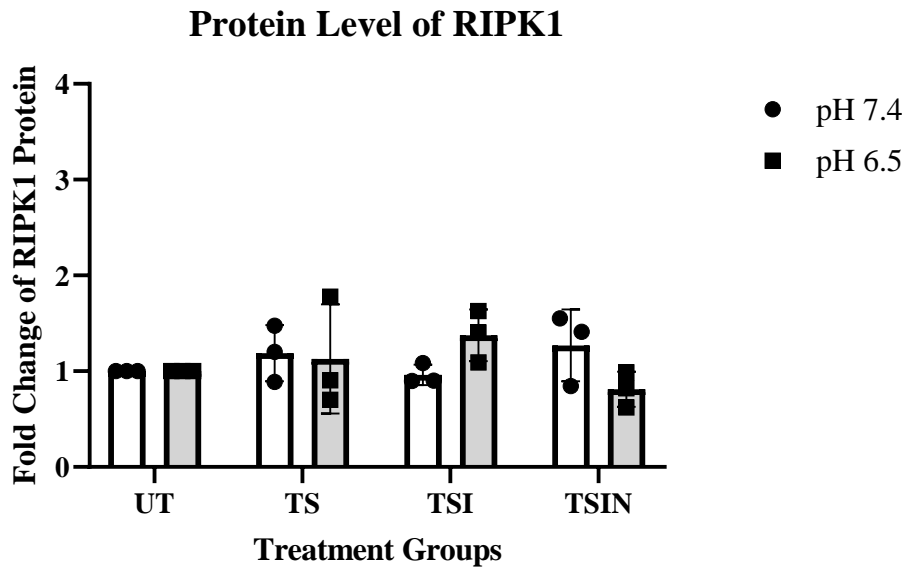
- (A) Cell death was analyzed using flow cytometry by staining for Annexin V and propidium iodide.
- (B) Quantification of cell death from flow cytometry results were calculated,  $n=3$ ; \* $p \leq 0.0332$ , \*\*\* $p \leq 0.0002$ , \*\*\*\* $p \leq 0.0001$ . Data is represented as mean  $\pm$  SD. 1-way ANOVA; Tukey's multiple comparisons test.

### 3.2 RIPK1 Function Is Unchanged at Acidic Conditions

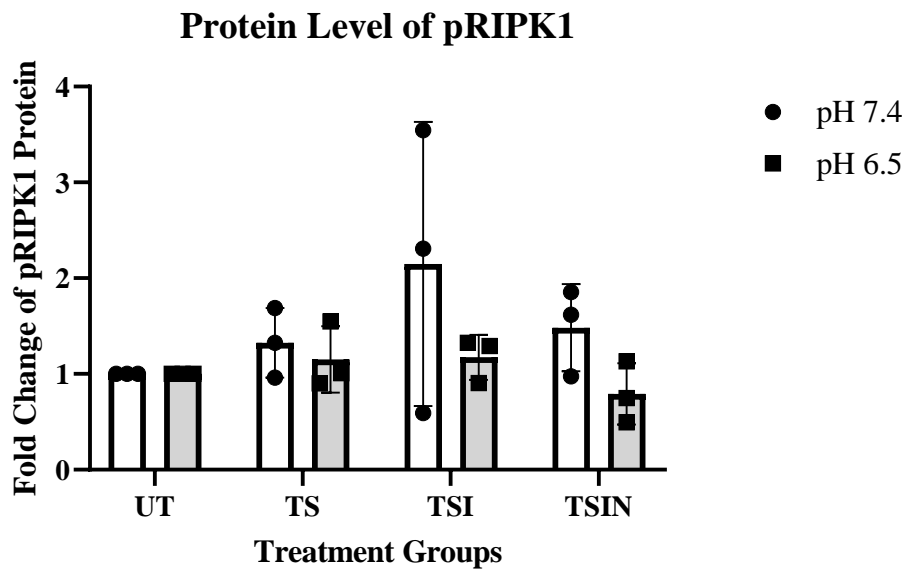
As measurements of cell death using the Incucyte and flow cytometry showed that necroptosis was inhibited at acidic pH, it was important to see if mediators of necroptosis were also affected due to the acidic cellular environment, specifically with regards to RIPK1. In the pathway of necroptosis, RIPK1 becomes phosphorylated and complexes with RIPK3 before leading to MLKL oligomerization<sup>68,77,86</sup>. As such, determining the relative protein levels or expression of RIPK1 and phosphorylated RIPK1 was completed to ascertain if changes in the environmental pH would impact expression and phosphorylation of RIPK1. Western blot analysis showed that both RIPK1 and pRIPK1 protein levels were not changed under acidic conditions compared to physiological pH (Figure 8). Hence, RIPK1 function remains unchanged despite changes in the extracellular and intracellular pH. This suggests that there may be other mechanisms which participate in the acidosis-regulated cell death shown in this study.

**A****Western Blot Following Death Assay at pH 7.4****B****Western Blot Following Death Assay at pH 6.5**

C



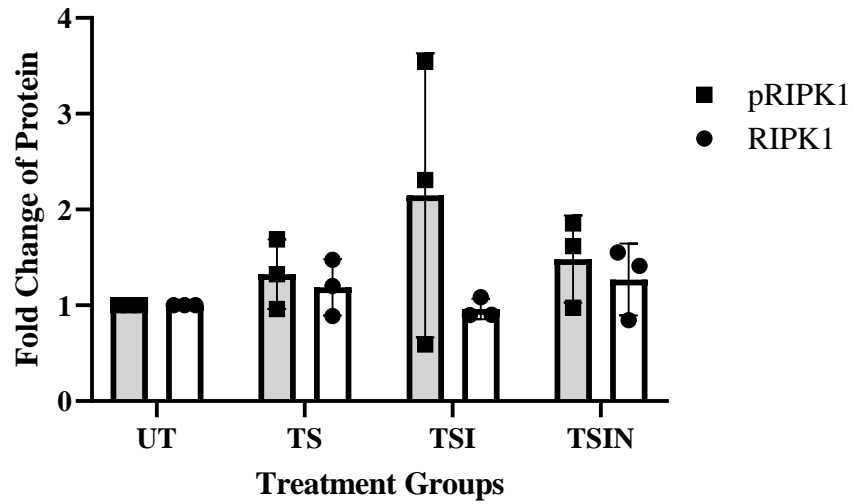
D





E

### Comparison of pRIPK1 and RIPK1 pH 7.4



F

### Comparison of pRIPK1 and RIPK1 pH 6.5

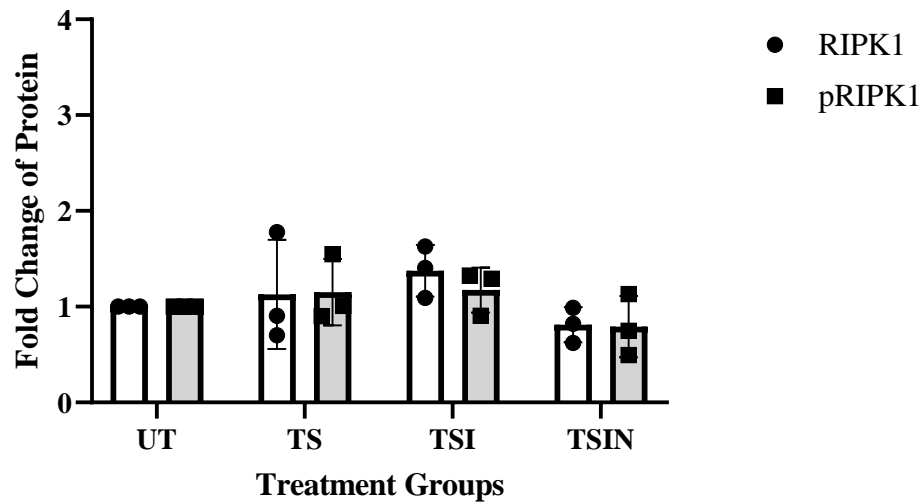


Figure 8: RIPK1 is not altered at acidic pH

WT MVECs were subjected to the cell death assay described earlier at pH 7.4 and 6.5 for 3 hours before total protein was isolated and western blot analysis was performed for the detection of RIPK1 and p-RIPK1 proteins. GAPDH was used as a loading control.

- (A) The protein levels of phosphorylated RIPK1 and total RIPK1 were confirmed by western blot analysis 3 hours after the death assay at pH 7.4. The band sizes are labelled and GAPDH was used as a loading control.
- (B) The protein levels of phosphorylated RIPK1 and total RIPK1 were confirmed by western blot analysis 3 hours after the death assay at pH 6.5. The band sizes are labelled and GAPDH was used as a loading control.
- (C) The relative expression of total RIPK1 was calculated with GAPDH as the baseline. The differences between treatment groups were not statistically significant, n=3; 1-way ANOVA and 2-way ANOVA; Tukey's multiple comparisons test.
- (D) The relative expression of phosphorylated RIPK1 was calculated with GAPDH as the baseline. The differences between treatment groups were not statistically significant, n=3; 1-way ANOVA and 2-way ANOVA; Tukey's multiple comparisons test.
- (E) The relative expression of phosphorylated RIPK1 to total RIPK1 with GAPDH as the baseline at pH 7.4. The differences between pRIPK1 and total RIPK1 as well as between treatment groups were not statistically significant, n=3; 2-way ANOVA; Tukey's multiple comparisons test.
- (F) The relative expression of phosphorylated RIPK1 to total RIPK1 with GAPDH as the baseline at pH 6.5. The differences between pRIPK1 and total RIPK1 as well as between treatment groups were not statistically significant, n=3; 2-way ANOVA; Tukey's multiple comparisons test.

### 3.3 Nuclear Translocation of AIF in Endothelial Cells is pH-Dependent

In apoptosis, the activation of the caspase cascade then triggers DNases which results in DNA fragmentation. Previous studies have shown that there is a caspase-independent mechanism for DNA fragmentation<sup>98,99,129</sup>. After the release of apoptosis-inducing factor (AIF) from the mitochondria into the cytosol, the molecule is truncated and then

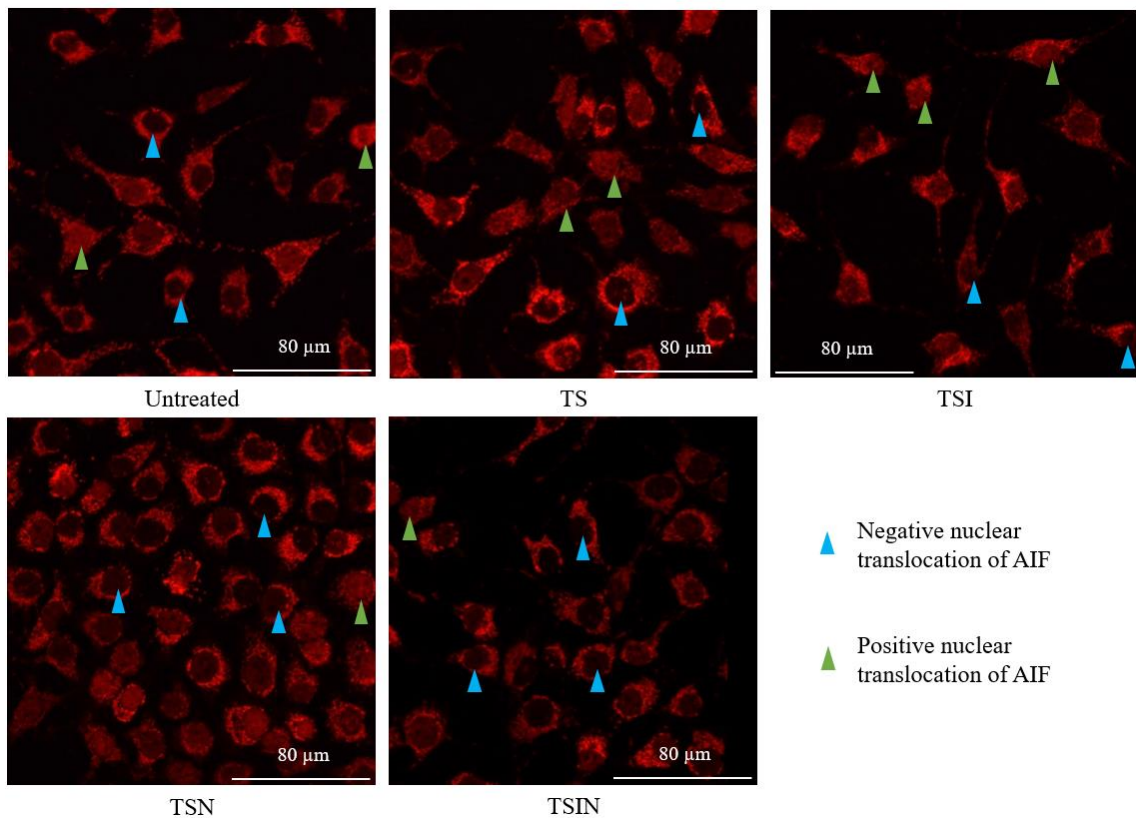
translocates into the nucleus alongside endonuclease G (EndoG) in order to cause large-scale DNA fragmentation and degradation<sup>91,97,99</sup>. We wanted to determine if AIF plays a role in cell death at acidic pH conditions and if so, whether EndoG is involved as well.

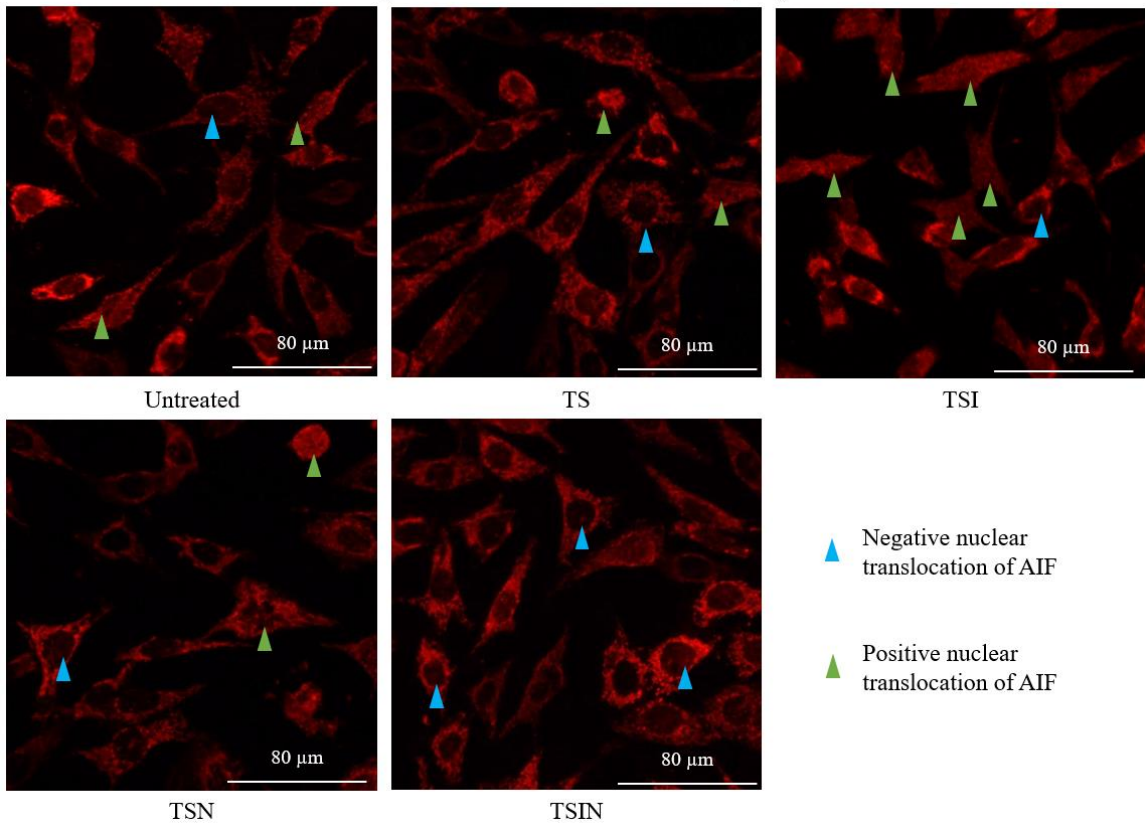
To confirm the role of AIF, WT endothelial cells were subjected to a death assay as described earlier and immunocytochemistry was used to observe AIF translocation into the nucleus in the different treatment groups, taking representative images of the wells for quantification (Figure 9A & 9B). The images were quantified for total cells and positive AIF nuclear translocation. Based on the representative images and quantification counts, the TSI treatment group had the highest level of positive AIF nuclear translocation at both pH 6.5 and 7.4 (Figure 9C & 9D). Overall, the amount of AIF nuclear translocation was upregulated in all the treatment groups at pH 6.5 compared to pH 7.4 (Figure 9E), suggesting that translocation of AIF may depend on the acidity of the cellular environment.

As AIF is implicated in DNA degradation following translocation into the nucleus, seeing whether the nuclear translocation could be inhibited to prevent cell death was of interest. Thus, WT endothelial cells were treated as described in section 2.3. To block AIF translocation at both pH 7.4 and 6.5, either 10-100  $\mu$ M of 3-ABA or 0.25-4  $\mu$ M of Alisporivir was added to the TS and TSI treatment groups to inhibit PARP-1 or CypA respectively. Based on the quantification of positive nuclear translocation, there was a significant reduction in nuclear translocation of AIF at pH 6.5 when 3-ABA or Alisporivir was added to the treatments (Figure 10). This suggests that AIF nuclear translocation can be controlled through the CypA/AIF complex or through parthanatos with PARP-1, which supports previous findings from other groups<sup>97,98,109,117,141</sup>.

A

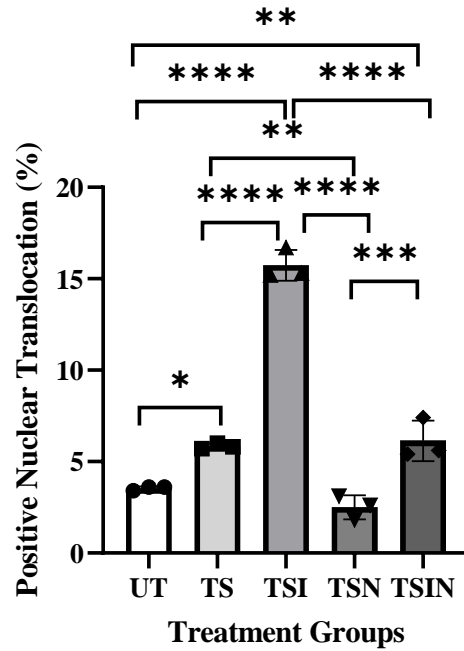
## Staining of AIF After 12 Hour Death Assay at pH 7.4



**B****Staining of AIF After 12 Hour Death Assay at pH 6.5**

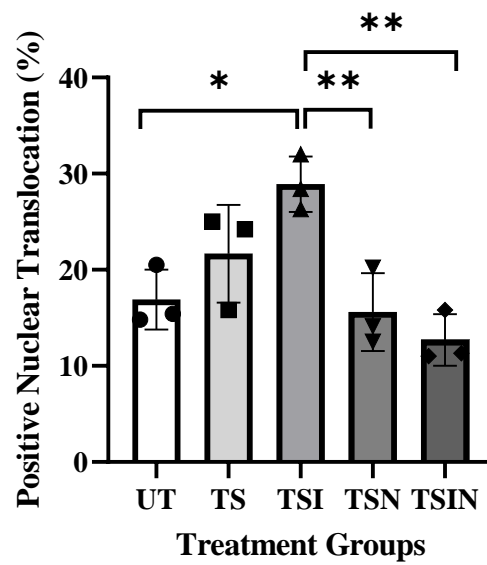
C

### Quantification of AIF Nuclear Translocation at pH 7.4



D

### Quantification of AIF Nuclear Translocation at pH 6.5



E

### Comparison of AIF Nuclear Translocation

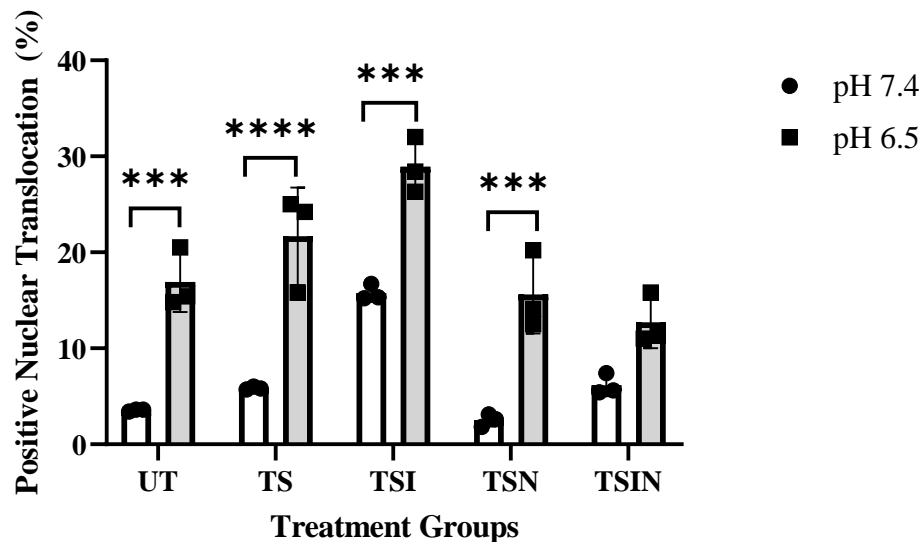


**Figure 9: Nuclear translocation of AIF in endothelial cells is pH-dependent**

WT MVECs were stained for AIF after death assays as described in section 2.3 with the addition of seeing whether using Alisporivir, a CypA inhibitor, and 3-ABA, a PARP-1 inhibitor, would impact nuclear translocation of AIF. Fluorescent images of each treatment were taken per well where each treatment had at least three wells of biological replicates and experiments were repeated thrice. Positive nuclear translocation was quantified.

- (A) Representative images of MVECs are shown following a death assay at pH 7.4. Representative positive AIF nuclear translocation is marked by the green arrowheads while absence of AIF nuclear translocation is marked by blue arrowheads.
- (B) Representative images of MVECs are shown following a death assay at pH 6.5. Representative positive AIF nuclear translocation is marked by the green arrowheads while absence of AIF nuclear translocation is marked by blue arrowheads.
- (C) Quantification of positive nuclear translocation at pH 7.4 after a 12-hour cell death assay and is representative of at least 3 independent experiments; n=3;

\*\*\*\* $p \leq 0.0001$ , \*\*\* $p \leq 0.0002$ , \*\* $p \leq 0.0021$ , \* $p \leq 0.0332$ , ns = non-significant (p-value  $\geq 0.05$ ); 1-way ANOVA; Tukey's multiple comparisons test.

**(D)** Quantification of positive nuclear translocation at pH 6.5 after a 12-hour cell death assay and is representative of at least 3 independent experiments; n=3;

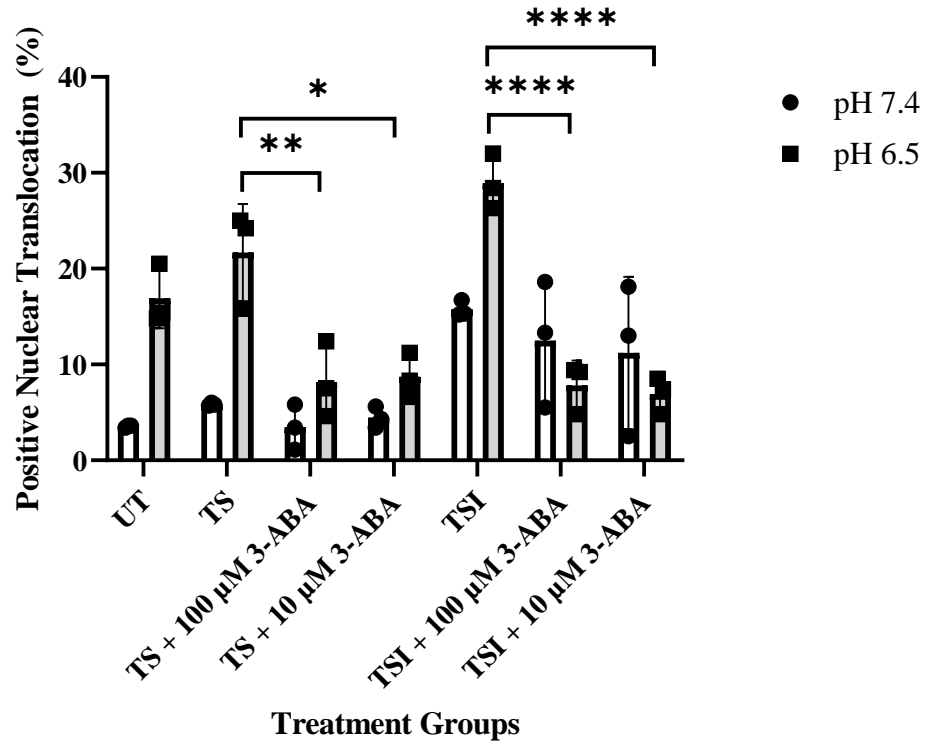
\*\*\*\* $p \leq 0.0001$ , \*\*\* $p \leq 0.0002$ , \*\* $p \leq 0.0021$ , \* $p \leq 0.0332$ , ns = non-significant (p-value  $\geq 0.05$ ); 1-way ANOVA; Tukey's multiple comparisons test.

**(E)** Quantification of positive nuclear translocation comparing pH 7.4 and pH 6.5 is representative of at least 3 independent experiments; n=3; \*\*\*\* $p \leq 0.0001$ ,

\*\*\* $p \leq 0.0002$ , \*\* $p \leq 0.0021$ , \* $p \leq 0.0332$ , ns = non-significant (p-value  $\geq 0.05$ ); 2-way ANOVA; Tukey's multiple comparisons test.



A

**Comparison of AIF Nuclear Translocation with PARP-1 Inhibition**

B

### Comparison of AIF Nuclear Translocation with CypA Inhibition

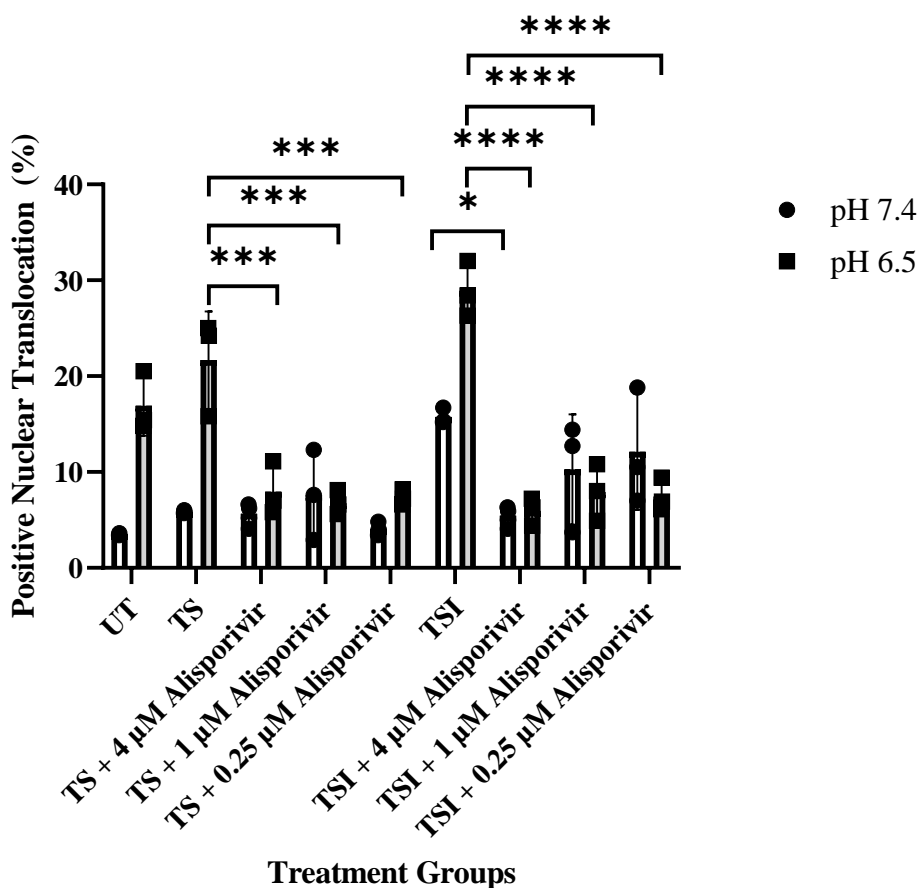


**Figure 10: PARP-1 and CypA inhibition reduces nuclear translocation of AIF at acidic pH conditions**

MVECs were treated to the death assays described in section 2.3 and varying concentrations of 3-aminobenzamide (3-ABA), a PARP-1 inhibitor, and Alisporivir, a CypA inhibitor, were added to the TS and TSI treatment groups.

(A) Quantification of positive nuclear translocation comparing pH 7.4 and pH 6.5 with the addition of 3-ABA is representative of at least 3 independent experiments;  $n=3$ ; \*\*\*\* $p \leq 0.0001$ , \*\* $p \leq 0.0021$ , \* $p \leq 0.0332$ , ns = non-significant ( $p$ -value  $\geq 0.05$ ); 2-way ANOVA; Tukey's multiple comparisons test.

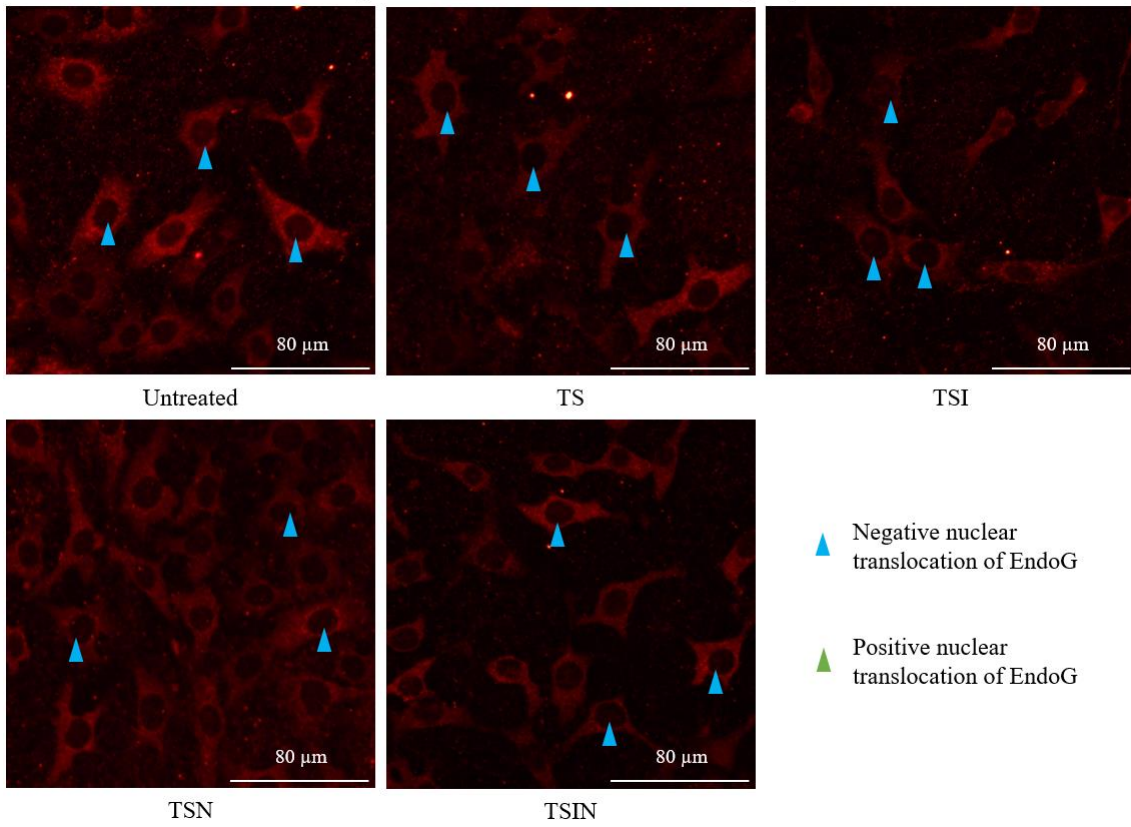
**(B)** Quantification of positive nuclear translocation comparing pH 7.4 and pH 6.5 with the addition of Alisporivir is representative of at least 3 independent experiments; n=3; \*\*\*\*p $\leq$ 0.0001, \*\*\*p $\leq$ 0.0002, \*p $\leq$ 0.0332, ns = non-significant (p-value  $\geq$  0.05); 2-way ANOVA; Tukey's multiple comparisons test.

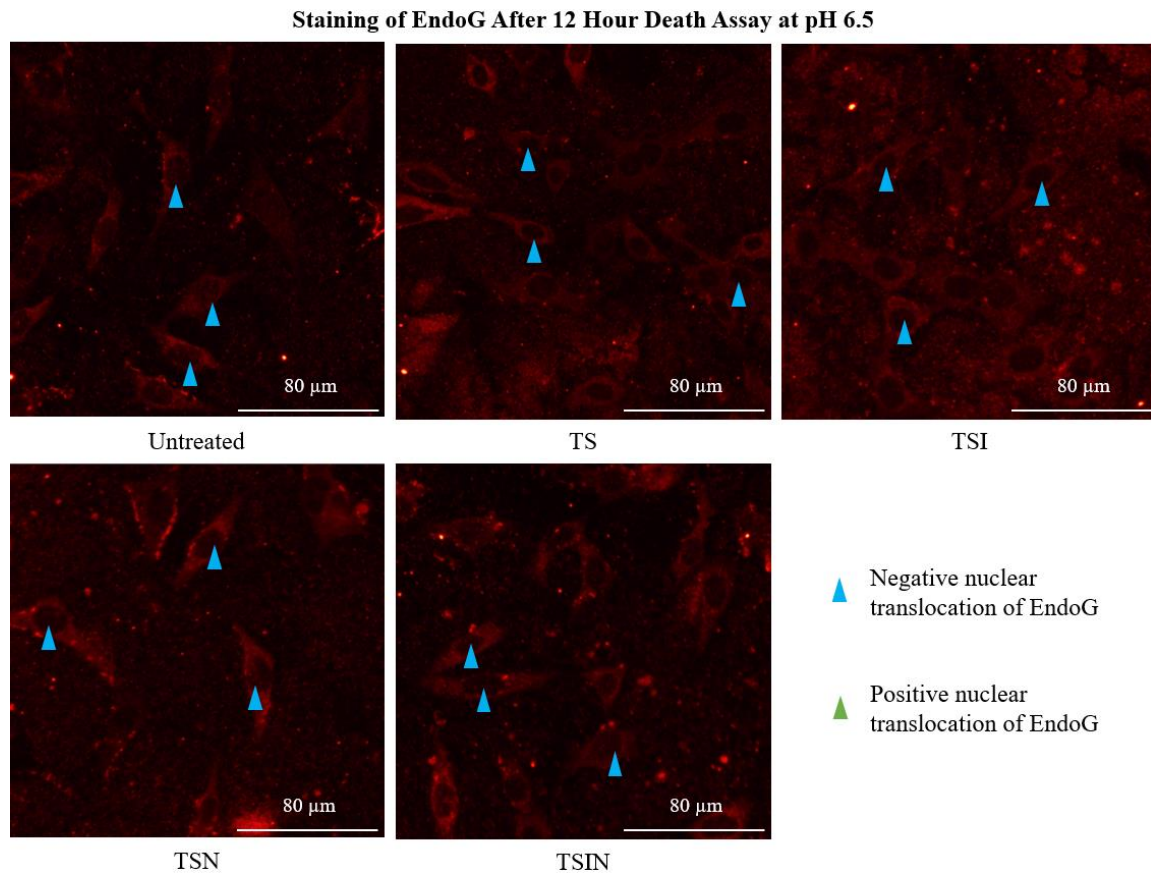
### 3.4 Endonuclease G Does Not Participate in Translocation of AIF at Acidic Conditions

While AIF has been implicated in DNA degradation and chromatin condensation, the molecule itself does not have intrinsic nuclease properties<sup>121,124,125</sup>. However, it was previously reported that endonuclease G (EndoG) and AIF can be released together from the mitochondria to move into the nucleus, causing DNA fragmentation<sup>99,116,122,97</sup>. To determine whether this is the case in acidic pH conditions, WT endothelial cells were subjected to a death assay as described earlier and immunocytochemistry was used to observe EndoG translocation into the nucleus in the different treatment groups, taking representative images of the wells for quantification. From the images taken, there was no nuclear translocation of EndoG present in either pH 7.4 or 6.5 (Figure 11). This suggests that there may be another nuclease interacting with AIF to cause DNA fragmentation.

A

## Staining of EndoG After 12 Hour Death Assay at pH 7.4



**B**

**Figure 11: Endonuclease G does not translocate into the nucleus at pH 7.4 and 6.5**

WT MVECs were stained for EndoG after death assays as described in section 2.3. Fluorescent images of each treatment were taken per well where each treatment had at least three wells of biological replicates and experiments were repeated thrice. Positive nuclear translocation of EndoG was not seen.

- (A) Representative images of MVECs are shown following a death assay at pH 7.4. Absence of EndoG nuclear translocation is marked by blue arrowheads.
- (B) Representative images of MVECs are shown following a death assay at pH 6.5. Absence of EndoG nuclear translocation is marked by blue arrowheads.

### 3.5 AIF Induces DNA Fragmentation in Endothelial Cells at Acidic Conditions

To gain a clearer understanding of AIF's role in acid-induced cell death, WT MVECs were subjected to the cell death assay described above at pH 6.5 and lysed for DNA. AIF has been associated with parthanatos, moving from the mitochondria into the nucleus due to the release of PAR polymers<sup>97,106</sup>. It has also been shown that CypA associates with AIF in the cytosol before translocating into the nucleus<sup>97,141</sup>. As a result, the addition of 3-ABA was used to determine if the inhibition of PARP-1 would play a role in cell death at acidic conditions. Furthermore, Alisporivir was added to determine if inhibition of AIF migration by blocking CypA would prevent DNA damage. Cell death was induced as described above and cell pellets were collected for DNA purification. DNA degradation was characterized through gel electrophoresis. In the images taken of the gels, there was a repetitive small-band nuclear fragmentation pattern visible in the treatment groups at pH 6.5 (Figure 12A) which was absent when 3-ABA or Alisporivir were added (Figure 12B & 12C). In conclusion, we have found that AIF causes small size DNA fragmentation which can be inhibited by blocking either the CypA/AIF complex or PARP-1.

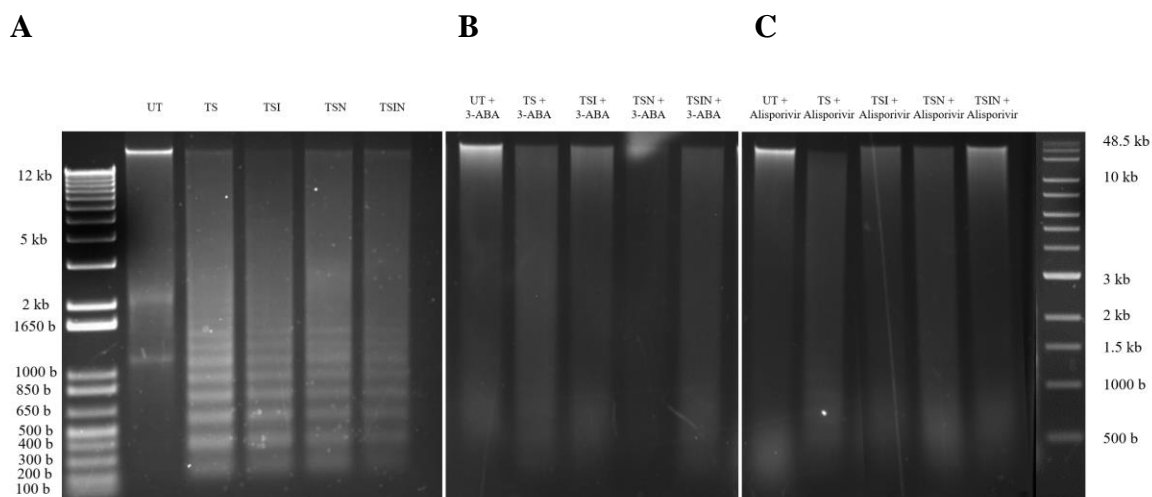


**Figure 12: Effects of PARP-1 and CypA inhibitors on DNA fragmentation at acidic pH conditions**

WT MVECs were subjected to the cell death assay previously mentioned at pH 6.5 for up to 45 hours before DNA was isolated with a phenol-chloroform extraction. DNA was quantified and run on an electrophoresis gel before being stained with a DNA gel and imaged.

- (A) WT MVECs were treated with the cell death assay previously mentioned at pH 6.5 for up to 45 hours, after which DNA was isolated and run on an electrophoresis gel. Image is representative of three independent experiments.
- (B) WT MVECs were treated with the cell death assay previously mentioned at pH 6.5 for up to 45 hours with the addition of 50  $\mu$ M 3-ABA to each treatment group, after which DNA was isolated and run on an electrophoresis gel. Image is representative of three independent experiments. The concentration of 50  $\mu$ M 3-ABA was selected because it was the lowest concentration with the most statistically significant change in cell death in the dose-response assay that will be discussed in section 3.7.
- (C) WT MVECs were treated with the cell death assay previously mentioned along with the addition of 4  $\mu$ M Alisporivir to each treatment group at pH 6.5 for up to 45 hours, after which DNA was isolated and run on an electrophoresis gel. Image is representative of three independent experiments. The concentration of 4  $\mu$ M

Alisporivir was chosen because it had the most statistically significant change in cell death in the dose-response assay that will be discussed in section 3.7.

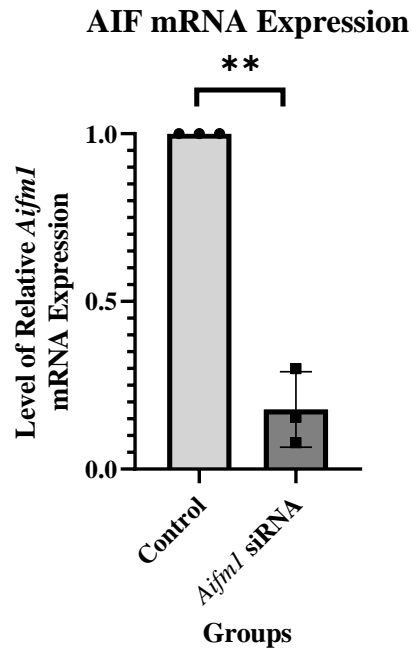
### 3.6 AIF Silencing Did Not Prevent Cell Death at Acidic pH

Currently, there are no pharmacological inhibitors which directly target AIF available<sup>117</sup>. As a result, to study the role of AIF in cell death at acidic conditions, the *Aifm1* gene was silenced in wild-type B6 endothelial cells using siRNA transfected into the cells for 24 hours. This silencing was confirmed through RT-qPCR and western blot (Figure 13A and 13C).

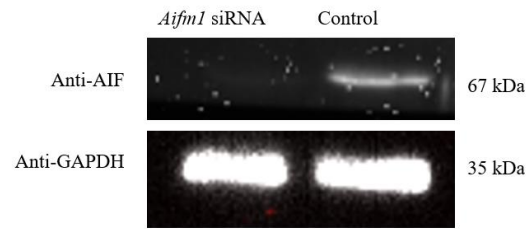
Silenced MVECs which were transfected with siRNA for 24 hours and control MVECs which were not transfected with siRNA were subjected to the death assays described earlier at pH 6.5 (Figure 14A and 14B). In comparing the silenced and control groups at pH 6.5, the silenced cells showed an increase in cell death when compared to control MVECs (Figure 14C).



A



B



C

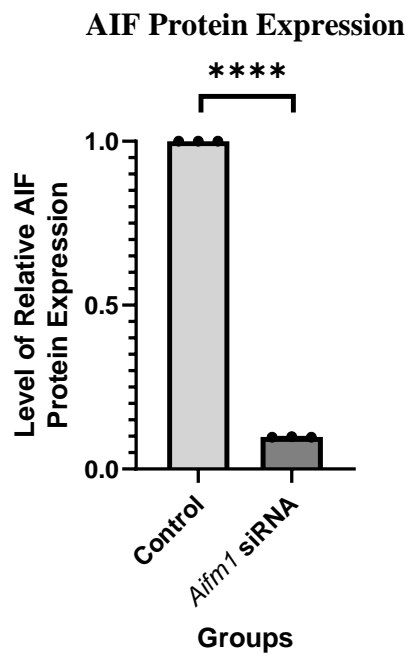
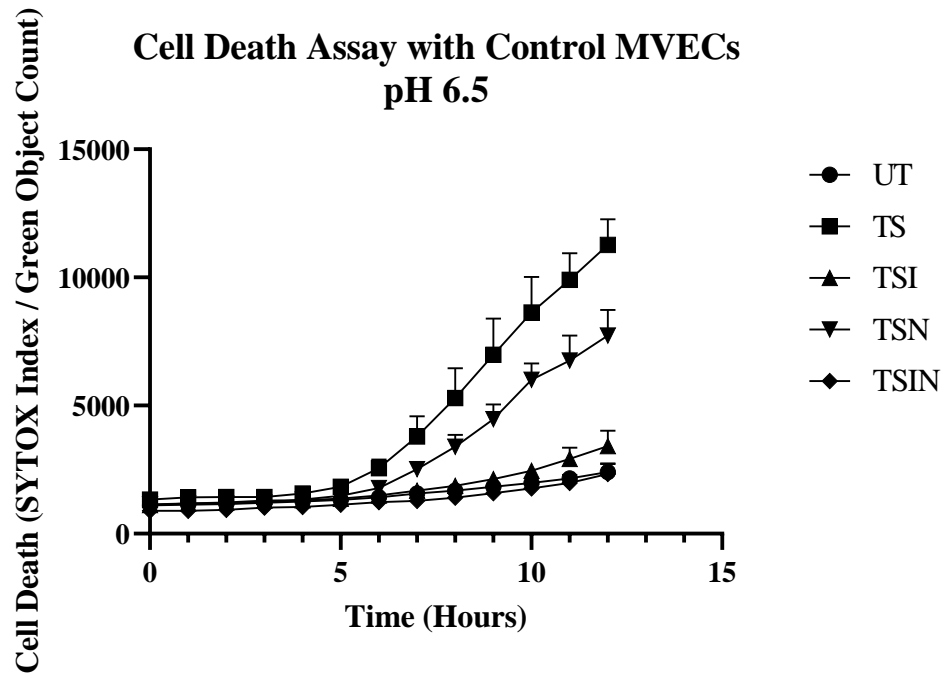


Figure 13: Confirmation of siRNA-induced silencing of *Aifm1* in endothelial cells

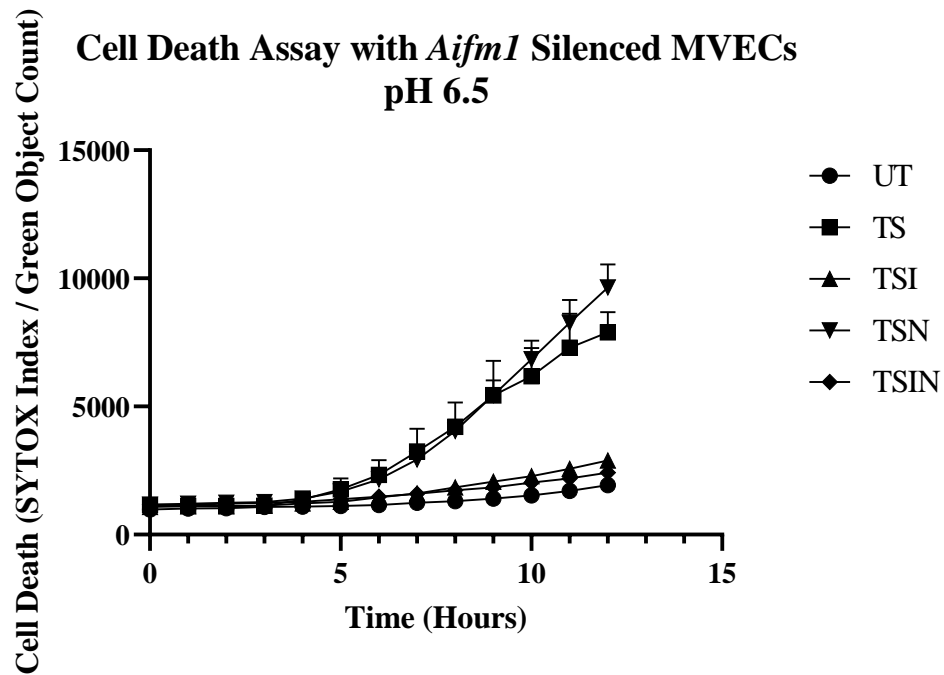
Wild-type MVECs were transfected with 50 nM of *Aifm1* siRNA using EndoFectin Max™ transfection reagent in Opti-MEM™ media for 24 hours.

- (A) The level of AIF mRNA expression was quantified in wild-type and siRNA silenced MVECs by RT-qPCR.  $\beta$ -actin was used as an endogenous control. Data are shown as mean  $\pm$  SD and representative of at least 3 independent experiments; n=3; \*\* $p \leq 0.0021$ ; Student's t-test for paired values.
- (B) The reduction in protein expression of AIF-silenced cells was confirmed by western blot analysis 24 hours after transfection. GAPDH was used as a loading control.
- (C) The level of AIF protein expression after 24 hours siRNA transfection was measured in 3 independent experiments; n=3, \*\*\*\* $p \leq 0.0001$ ; Student's t-test for paired values.

A



B



C

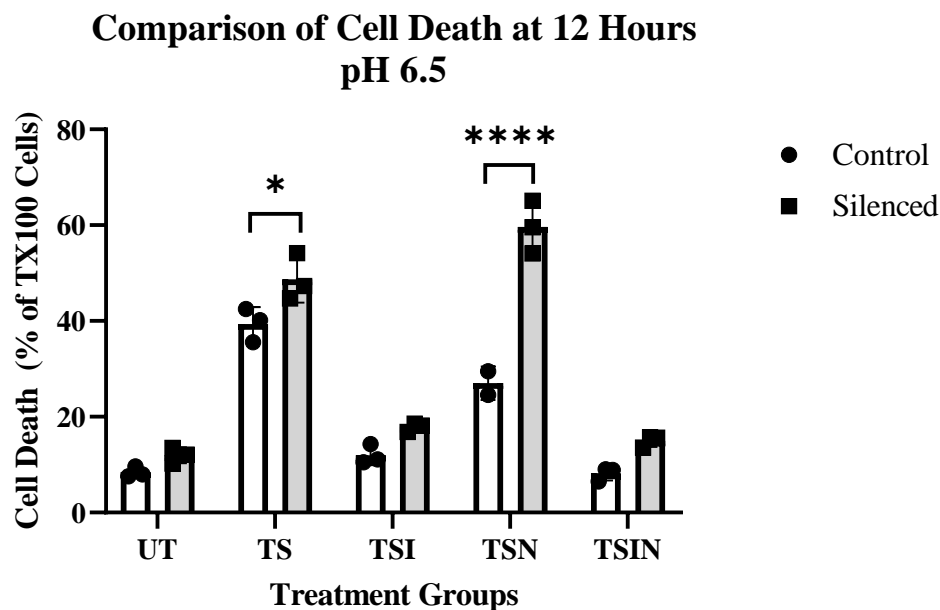


**Figure 14: AIF siRNA-induced silencing increased cell death**

WT MVECs were transfected with siRNA or with EndoFectin Max only for 24 hours before being plated on 96-well plates and treated as described earlier. Data at 12 hours following the start of the death assay are shown as mean  $\pm$  SD and representative of at least 3 independent experiments.

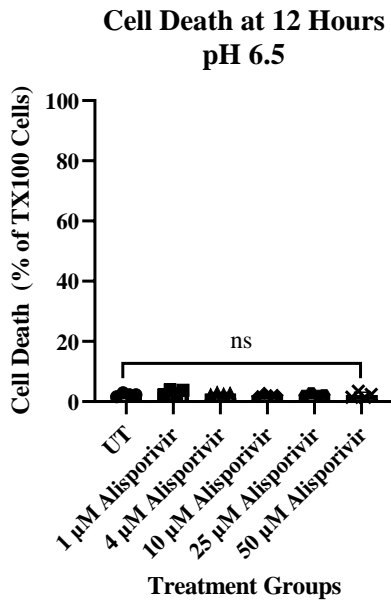
- (A) Control MVECs were harvested 24 hours post-transfection and subjected to the death assay at pH 6.5 as previously mentioned in section 2.3.2 in triplicate. As a positive control (not shown), 0.1% Triton™ X-100 (TX100), a non-ionic surfactant was used to induce 100% cell death and to calculate the percent of cell death in all treatments.
- (B) *Aifm1* silenced MVECs were harvested 24 hours post-transfection and subjected to the death assay at pH 6.5 as previously mentioned in section 2.3.2 in triplicate. As a positive control (not shown), 0.1% Triton™ X-100 (TX100), a non-ionic surfactant was used to induce 100% cell death and to calculate the percent of cell death in all treatments.
- (C) Data at 12 hours from the start of the death assay at pH 6.5 comparing the levels of cell death between *Aifm1* silenced MVECs and control MVECs are shown as mean  $\pm$

SD and representative of at least 3 independent experiments; n=3; \*\*\*\*p≤0.0001, \*p≤0.0332, ns = non-significant (p-value ≥ 0.05); 2-way ANOVA; Tukey's multiple comparisons test.

### 3.7 Cyclophilin A is Modestly Involved in Endothelial Cell Death at Acidic Conditions

In PCD, tAIF translocates from the mitochondria to the nucleus, which is positively regulated by cytosolic CypA<sup>97,98,116,117,121,124,126,127,130,141</sup>. This translocation then leads to chromatinolysis and DNA degradation caused by an associated nuclease. In the nucleus, the truncated form of AIF associates with phosphorylated histone H2AX ( $\gamma$ H2AX) and CypA, or endonuclease G (EndoG) to provoke chromatin condensation and DNA degradation in AIF-mediated necroptosis<sup>97,98,121,125-127,130</sup>. Since there was a significantly higher level of AIF nuclear translocation at pH 6.5 in all the treatment groups compared to pH 7.4, it was of interest to see whether endothelial cell death at acidic pH conditions was altered with the inhibition of cyclophilin A. Alisporivir was added to the following treatments at pH 6.5: untreated [UT]; and TNF- $\alpha$  + SMAC mimetic [TS], which represents apoptosis. Interestingly, the addition of Alisporivir to the TS treatment group led to a small but significant increase in cell death at pH 6.5 (Figure 15). While this suggests that CypA may be involved in endothelial cell death, it also raises the possibility that inhibition of the CypA-AIF complex due to Alisporivir instead shifts the cell death mechanism to a different pathway or other molecules also participate cell death since cell death was not completely inhibited.

A



B

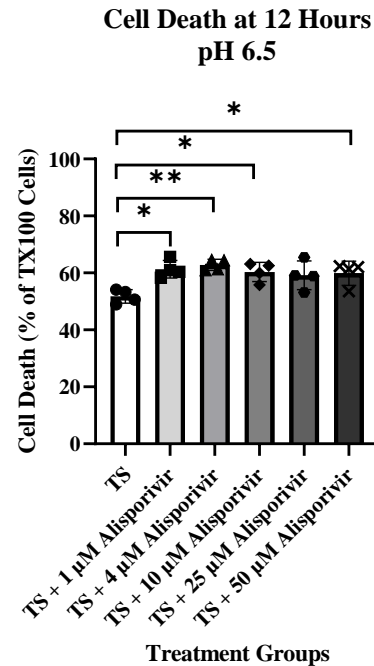


**Figure 15: Cyclophilin A is modestly involved in endothelial cell death at acidic pH conditions**

WT MVECs were subjected to the death assay described earlier in sections 2.3.2 and 3.1. The cyclophilin A inhibitor, Alisporivir, was added at concentrations ranging from 1 to 50  $\mu$ M to block AIF nuclear translocation and the CypA-AIF interaction.

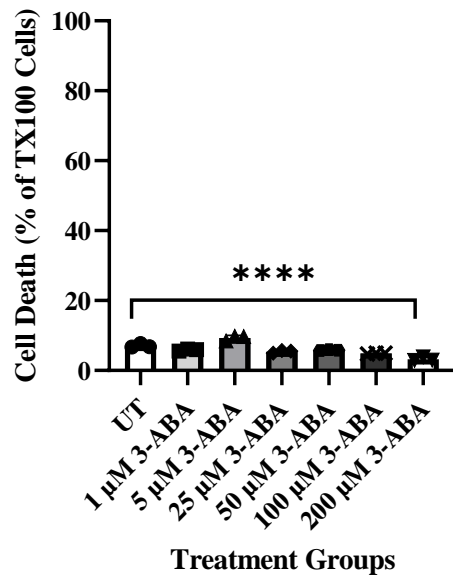
- (A) Data at 12 hours from the start of the death assay at pH 6.5 for untreated and 1-50  $\mu$ M Alisporivir are shown as mean  $\pm$  SD and representative of at least 3 independent experiments; n=4; ns = non-significant (p-value  $\geq$  0.05); 1-way ANOVA; Tukey's multiple comparisons test.
- (B) Data at 12 hours from the start of the death assay at pH 6.5 for TS and TS + 1-50  $\mu$ M Alisporivir are shown as mean  $\pm$  SD and representative of at least 3 independent experiments; n=4; \*p $\leq$ 0.0332, ns = non-significant (p-value  $\geq$  0.05); 1-way ANOVA; Tukey's multiple comparisons test.

### 3.8 Parthanatos May Be Involved in Endothelial Cell Death at Acidic Conditions

As previously mentioned, parthanatos consists of the overexpression of poly (ADP-ribose) polymerase 1 or PARP-1, which leads to cell death and DNA damage. This includes translocation of nuclear PAR polymers to the mitochondria causing AIF release and cell death. The role of parthanatos was investigated in acid-induced endothelial cell death using a PARP-1 inhibitor, 3-aminobenzamide or 3-ABA, which was added to the cells with the following treatments: untreated [UT]; TNF- $\alpha$  + SMAC mimetic [TS], which should represent apoptosis; and TNF- $\alpha$  + SMAC mimetic + z-IETD-fmk [TSI], which should represent necroptosis. The addition of 3-ABA to untreated cells showed a reduction in apoptotic cell death at 12 hours at pH 7.4 (Figure 16A) while the addition of 3-ABA to untreated cells at pH 6.5, TS treated cells at pH 6.5 and pH 7.4, and TSI treated cells at pH 7.4 did not show a significant reduction in cell death at 12 hours with the highest concentration of 3-ABA. However, the addition of 3-ABA to TSI treated cells showed a statistically significant reduction in cell death at 12 hours for pH 6.5 (Figure 16F).

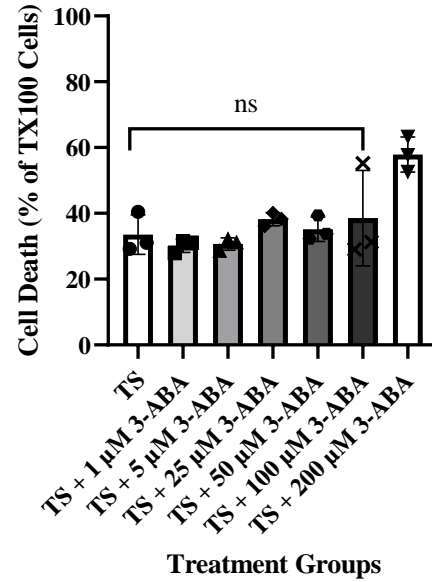
A

Cell Death at 12 Hours  
pH 7.4



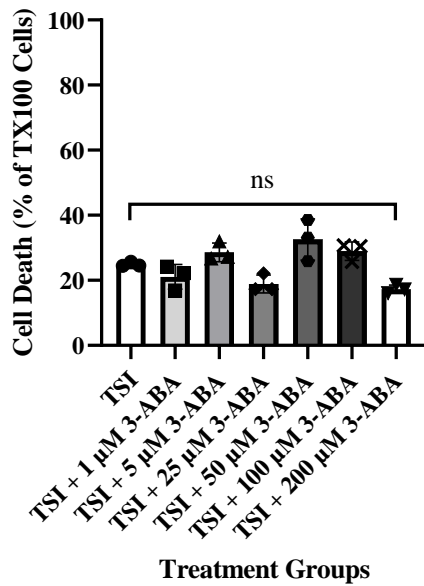
B

Cell Death at 12 Hours  
pH 7.4



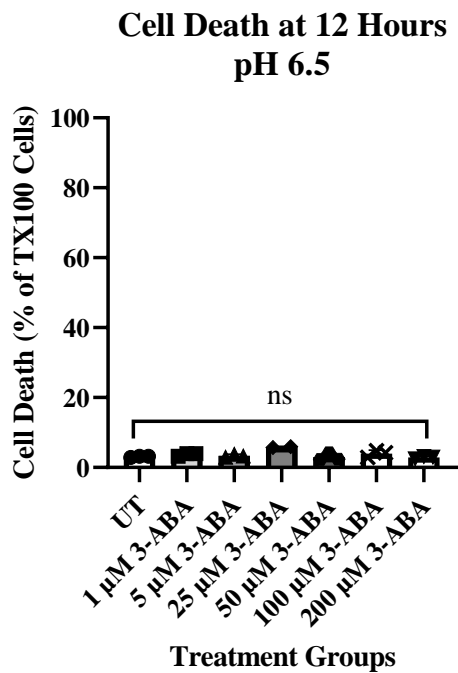
C

Cell Death at 12 Hours  
pH 7.4

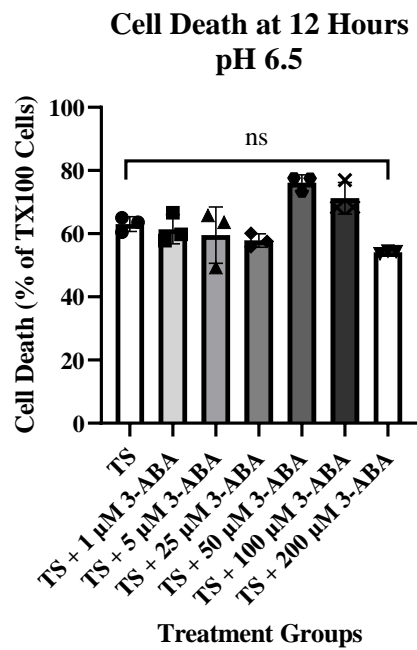




D



E



F

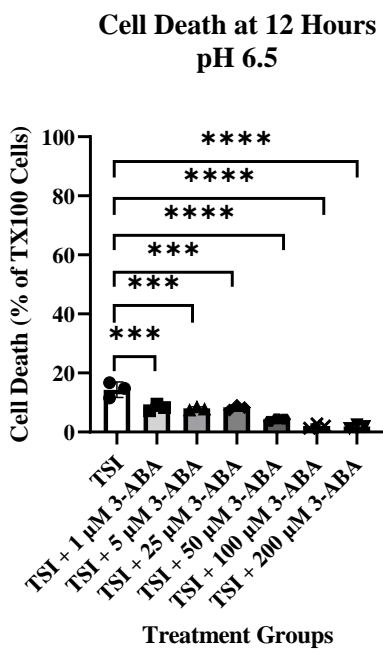


**Figure 16: Parthanatos may contribute to endothelial cell death**

WT MVEC's were subjected to the death assay described earlier in sections 2.3.2 and 3.1. The PARP-1 inhibitor, 3-ABA, at concentrations ranging from 1-200  $\mu\text{M}$ , was added to block parthanatos.

- (A) Data at 12 hours from the start of the death assay at pH 7.4 for untreated and 1-200  $\mu\text{M}$  3-ABA are shown as mean  $\pm$  SD and representative of at least 3 independent experiments;  $n=3$ ;  $**p \leq 0.0021$ ,  $*p \leq 0.0332$ , ns = non-significant ( $p\text{-value} \geq 0.05$ ); 1-way ANOVA; Tukey's multiple comparisons test.
- (B) Data at 12 hours from the start of the death assay at pH 7.4 for TS and TS + 1-200  $\mu\text{M}$  3-ABA are shown as mean  $\pm$  SD and representative of at least 3 independent experiments;  $n=3$ ;  $**p \leq 0.0021$ , ns = non-significant ( $p\text{-value} \geq 0.05$ ); 1-way ANOVA; Tukey's multiple comparisons test.
- (C) Data at 12 hours from the start of the death assay at pH 7.4 for TSI and TSI + 1-200  $\mu\text{M}$  3-ABA are shown as mean  $\pm$  SD and representative of at least 3 independent experiments;  $n=3$ ;  $**p \leq 0.0021$ ,  $*p \leq 0.0332$ , ns = non-significant ( $p\text{-value} \geq 0.05$ ); 1-way ANOVA; Tukey's multiple comparisons test.
- (D) Data at 12 hours from the start of the death assay at pH 6.5 for untreated and 1-200  $\mu\text{M}$  3-ABA are shown as mean  $\pm$  SD and representative of at least 3 independent experiments;  $n=3$ ; ns = non-significant ( $p\text{-value} \geq 0.05$ ); 1-way ANOVA; Tukey's multiple comparisons test.
- (E) Data at 12 hours from the start of the death assay at pH 6.5 for TS and TS + 1-200  $\mu\text{M}$  3-ABA are shown as mean  $\pm$  SD and representative of at least 3 independent experiments;  $n=3$ ;  $*p \leq 0.0332$ , ns = non-significant ( $p\text{-value} \geq 0.05$ ); 1-way ANOVA; Tukey's multiple comparisons test.
- (F) Data at 12 hours from the start of the death assay at pH 6.5 for TSI and TSI + 1-200  $\mu\text{M}$  3-ABA are shown as mean  $\pm$  SD and representative of at least 3 independent experiments;  $n=3$ ; ns = non-significant ( $p\text{-value} \geq 0.05$ ); 1-way ANOVA; Tukey's multiple comparisons test.

## Chapter 4

### 4 Discussion

#### 4.1 Study Summary

Solid organ transplantation remains one of the best treatment courses for end-stage organ failure<sup>56,64</sup>. Furthermore, forms of cell death such as apoptosis and necroptosis have been shown to play an important role in the pathogenesis of clinical conditions and diseases<sup>77</sup>. Understanding apoptosis and necroptosis pathways in the context of organ transplantation may provide information to improve or prolong the success of transplants. Apoptosis is a well-defined cell death pathway which can be induced by death receptors or by MOMP and caspases<sup>67,77</sup>. Necroptosis is a form of caspase-independent cell death which causes inflammation, contributing to graft injury and an immune response<sup>56,66,68,77,88</sup>. Previous work by our group has demonstrated the role of necroptosis causing inflammation and injury in heart and kidney grafts<sup>46,131,142,143</sup>. RIPK1 and RIPK3 have been shown to be involved in necroptosis and that inhibition of RIPK3 reduced graft rejection<sup>131,143</sup>. In addition to this, we have also shown that cyclophilin D (CypD), a MPTP regulator molecule, is a promising target in the downstream pathway of TNF- $\alpha$  mediated necroptosis in two different *in vitro* models with various treatment groups – one using physiological pH and another using cold hypoxia-reoxygenation injury<sup>132,142</sup>. Transplant survival was also prolonged in heterotopic transplantation using CypD<sup>-/-</sup> hearts compared to wild-type hearts<sup>132,142</sup>. The earlier pathways of TNFR1-induced necroptosis have been carefully outlined and studied, but there is some debate as to the mechanisms involved at the end of the pathway and the involvement of the mitochondria<sup>68,77,83,86,116</sup>. As such, having learned that cyclophilin D is a potential target in necroptosis, it was clear that downstream mediators of CypD-mediated mPTP formation required investigation to gain a clearer picture of the downstream necroptotic pathway.

During ischemia when blood flow is interrupted or absent, cells switch to anaerobic metabolism and generate lactic acid, causing a subsequent drop in intracellular pH<sup>33,40,42,47</sup>. In this study, we investigated the role of necroptosis in cell death, controlling for the pH of the surrounding cellular environment to represent the acidic conditions

which occur in ischemia. We demonstrated that the level of necroptotic cell death was reduced in acidic extracellular pH. Furthermore, nuclear translocation of AIF can be upregulated by low pH while causing large-scale DNA fragmentation and apoptotic laddering. Finally, parthanatos may be involved in endothelial cell death at physiological and acidic pH. Targeting AIF to prevent its nuclear translocation may be a potential approach for therapeutic strategies to reduce IRI and improve graft function in transplantations.

#### 4.1.1 The Endothelium in Organ Transplantation

The endothelium is important in maintaining vascular homeostasis and is the first contact site between immune system of the recipient and the foreign cells from the donor organ in transplantations<sup>61,64,65,95</sup>. This barrier helps to regulate the movement of immune cells in and out of the organ, protecting the allograft from pathogens<sup>62-65</sup>. The endothelium is susceptible to damage and injury during ischemia and reperfusion, which can lead to dysfunctions in the balance between vasodilation and vasoconstriction, blood flow, and promote inflammation and alloimmunity<sup>58,64,65,95</sup>. These changes can lead to graft injury and necrosis, causing programmed cell death induced by IRI<sup>58,64</sup>. Knowing that the endothelium is a crucial barrier, it is important to target endothelial cells to prevent cell death and damage following transplants.

#### 4.1.2 Necroptosis in IRI and Organ Transplantation

IRI are unavoidable consequences of the transplantation process which can have detrimental effects on the long-term success of the allograft leading to graft rejection<sup>34,40,47</sup>. There have been advances in organ storage and preservation using machinery to reduce IRI but limited research in targeting molecular mediators of IRI associated with various forms of PCD<sup>5,6,12,66,144</sup>. Understanding the mechanisms and role of various ligands in PCD could lead to methods specifically targeting IRI which will improve graft survival.

Numerous studies reported that organ damage post-ischemia and reperfusion is mainly mediated by inflammation, apoptosis, and necroptosis<sup>42,55,88,90,93</sup>. In the recent work published by our group, endothelial cells were shown to be susceptible to TNFR1-

mediated necroptosis and that targeting mediators of necroptosis (RIPK1 and RIPK3) led to prolonged graft survival of heterotopic heart transplantations in mice<sup>131,142,143</sup>. Our studies were confirmed by recent publications that showed that necroptosis is a major contributor to injury in organ transplantation and is not only limited to cardiac transplants<sup>56,83,86,88,89</sup>. The involvement of TNFR1-mediated necroptosis was also confirmed in a hypoxia-reoxygenation model to mimic ischemia-reperfusion injury and that AIF nuclear translocation was shown in cells exposed to hypoxia-reoxygenation<sup>132</sup>. Thus, this current study was designed in order to better understand the role of AIF in cell death pathways as well as the downstream signalling involved.

#### 4.1.3 The Impact of Acidic pH on Necroptosis

Some studies have used cardiac myocytes to examine the changes in pH which occur during IRI. The environmental changes which occur with shifts in pH during IRI have been called a paradox, in part because the lowering of pH that results during ischemia and anaerobic metabolism does not impact the tissues as negatively as does the return of blood flow and restoration of physiological pH during reperfusion<sup>33,40</sup>. In some studies, the acidic cellular environment was shown to lead to an upregulation of apoptosis in tumor cells<sup>145</sup>. On the other hand, there has also been research which states lower acidic pH conditions can inhibit levels of apoptosis compared to physiological pH conditions<sup>146</sup>. While these suggest conflicting remarks about the impact that acidic pH conditions has on apoptotic cell death, it is possible that there are multiple pathways involved which control induction of apoptosis depending on the pH of the environment.

There have been limited studies on the effects of environmental pH on TNFR1-mediated necroptosis. Previous studies showed contradictory results on pH-regulated cell necroptosis. In one study, it was shown that RIPK1 is not cleaved under acidic pH conditions in HT29 cells, which may explain why RIPK1-dependent necrosis can occur at acidic conditions<sup>147</sup>. Another study suggested that when intracellular pH was basic due to osmotic stress, necroptosis was induced by directly activating RIPK3<sup>148</sup>. On the other hand, there have been studies reporting that acidic pH induces necrotic-like cell death<sup>147,149</sup>. One study published in 2020 showed similar results to this project with respect to the effects that acidic environmental conditions had on necroptotic cell

death<sup>150</sup>. In the study, the researchers found that proliferating T-lymphocyte cells which consumed sodium bicarbonate and released lactate led to a surrounding pH of 6.3 for the culture medium<sup>150</sup>. When this occurred, there was an inhibition of TNFR1-mediated necroptosis which was reversed when the environmental pH was neutralized, suggesting that like this project, the acidification of culture medium is critical for the inhibition of cell death<sup>150</sup>. The acidic extracellular pH was also shown to impair RIPK1 kinase activation and autophosphorylation at Ser166<sup>150</sup>. Thus, RIPK1 activation, necroptosis, and apoptosis were all inhibited at low pH<sup>150</sup>. In our current project, we were not able to show a statistically significant decrease in RIPK1 and its kinase activity at acidic pH conditions compared to physiological pH (Figure 8). However, from the western blot images taken of the protein levels of RIPK1 and p-RIPK1, there was a visual reduction in p-RIPK1 at pH 6.5 compared to pH 7.4 (Figure 8), which might potentially correlate with the study previously mentioned.

#### 4.1.4 Acid-Induced Cell Death Upregulates AIF Nuclear Translocation

The mechanism underlying the translocation of AIF in the context of cell death is not fully understood yet, but the general steps involved are first the truncation of AIF, followed by its exit from the mitochondria after membrane permeabilization. Previous studies have found potential molecules involved in the release of AIF such as PARP-1, Bax, or Bid<sup>106,109,110</sup>. In this study, we were able to show that PARP-1 may be involved in endothelial cell death at both physiological and acidic pH. When cells were treated at a low pH of 6.5, there was an increase in AIF nuclear translocation in all treatment groups compared to physiological pH of 7.4 (Figure 9E). However, there was a decrease in cell death when apoptosis was blocked at pH 6.5 compared to pH 7.4, where the pathway was shifted to necroptosis. Thus, it is possible that nuclear translocation of AIF is not positively correlated with necroptotic cell death. In addition to this, AIF has been labelled as a caspase-independent apoptosis inducer alongside endonuclease G, both having been implicated in necroptosis<sup>99</sup>. One study found that AIF and endonuclease G (EndoG) interact in the nucleus and that EndoG cleaves DNA<sup>99</sup>. In this project, immunocytochemistry experiments were also completed with anti-EndoG antibody.

However, staining of treated cells at physiological and acidic pH did not show nuclear translocation of EndoG (Figure 11). This suggests that other nucleases are involved in DNA degradation in our current model.

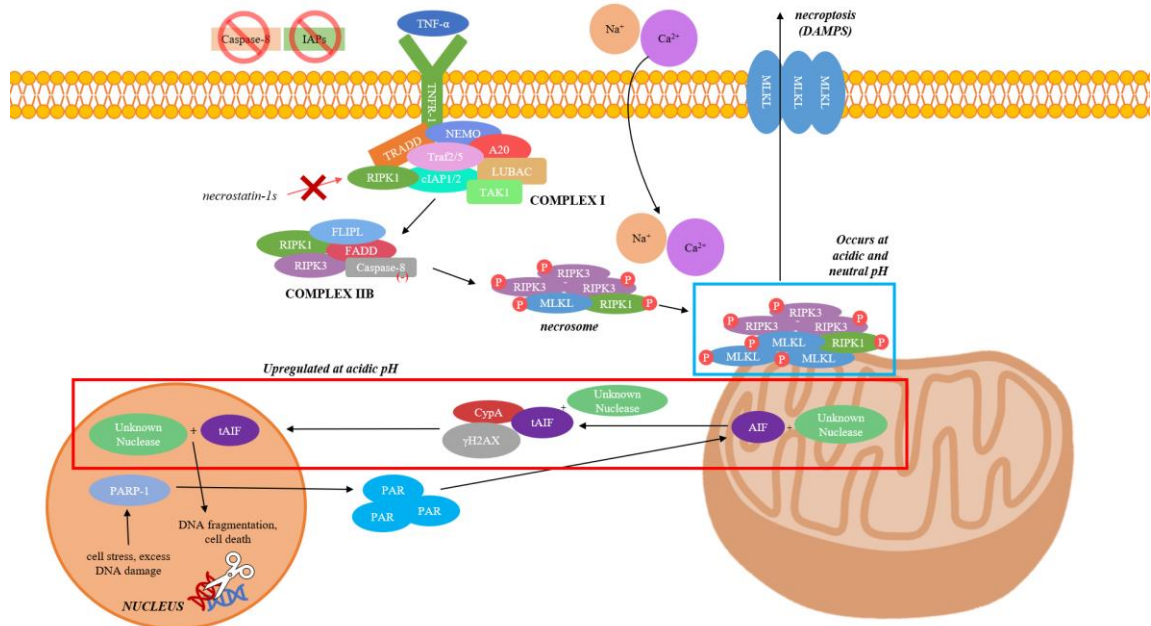


**Figure 17: Proposed mechanism of necroptosis in acidic pH conditions**

Based on the findings from this study, the function of RIPK1 is not affected by changes in pH of the extracellular environment. However, the nuclear translocation of AIF was shown to be upregulated at acidic pH conditions. Both PARP-1 and CypA inhibition led to a significant decrease in positive AIF nuclear translocation at acidic pH conditions, suggesting that both pathways may be involved in acidic cell death.

## 4.2 Future Directions

The fact that there was greater positive AIF translocation in the treatments at acidic pH suggests a potential upregulation of PARP-1 activity, releasing truncated AIF from the mitochondria before entering the nucleus. It will be interesting to define this mechanism in future. In addition, while AIF has been implicated in cell death when it translocates into the nucleus, it is also an essential molecule within the mitochondria<sup>116–118,121</sup>. It may not be possible to completely remove the presence of AIF within the cell due to adverse

effects, so a better approach might be to limit only the nuclear translocation of AIF with pharmacological agents such as Alisporivir *in vitro* and in a murine heart transplantation model.

While we were able to show that nuclear translocation of AIF was upregulated in an acidic environment and proceeded to large-scale DNA fragmentation, the enzyme or nuclease involved in the actual fragmentation of DNA was not found. As previously mentioned, in this project, EndoG did not migrate with AIF into the nucleus in the treatment groups at pH 6.5 and 7.4. Therefore, it would be worthwhile to investigate potential nucleases that are responsible for the large-scale DNA fragmentation that was seen in the treatments at pH 6.5. One suggested molecule to focus on would be macrophage migration inhibitory factor (MIF), which has been implicated in PARP-1 induced DNA fragmentation<sup>107,113</sup>. Another important next step would be to investigate the role of AIF in an *in vivo* murine cardiac transplantation model using AIF knockout mice. One model would be to use mice with the Harlequin (Hq) mutation, which causes an 80% reduction in AIF expression<sup>117,151</sup>.

### 4.3 Limitations

One limitation of the findings from this project is the exclusive use of an *in vitro* model using MVECs. Working with an isolated system such as the cell model that was used would not account for any physiological or pharmacological cellular responses in the external environment, including any interactions with other types of cells within the organ or body system. In this study, the condition of acidosis associated with ischemia was simulated by using acidic pH conditions *in vitro* with cell culture media. However, ischemia during transplantation is also the result of the deprivation of oxygen and blood flow, which were not factored into the model used for this project<sup>34,40,42,47,48,115</sup>.

Furthermore, when an organ – in this case, the heart – is removed and prepared for transplantation, the time that the organ is ischemic is limited as much as possible<sup>11,38,39</sup>. Typically, donor organs are subjected to no more than five hours of ischemia before they are transplanted into the recipient and reperfused with oxygenated blood<sup>35–37</sup>. In addition, the assays in the study only focussed on the cell death pathways of apoptosis and necroptosis. However, as previously mentioned, cell death mechanisms extend beyond



just the two pathways used in this project<sup>82,85</sup>. There are multiple factors and mechanisms that can lead to ischemia-reperfusion injury and inflammatory responses, so it is possible that there are other death pathways not addressed in this study, such as pyroptosis or ferroptosis, which also contribute to cardiac graft injury that were not a focus of this project<sup>85,102-104</sup>. As such, the results from the in vitro model may not accurately represent transplantation results from in vivo studies or reflect clinical conditions. Thus, there would be additional factors that were not accounted for in this model that could hinder the applicability of this work in a clinical setting.

An additional limitation was the methodology used in quantifying nuclear translocation of AIF. For this project, two separate individuals counted the amount of positive AIF translocation in a blinded manner. The criteria for positive and negative translocation were defined. However, there is greater potential for errors in counting by visual confirmation compared to the use of an imaging software that defines the threshold for translocation, something which should be considered for future experiments involving quantifying nuclear translocation. Finally, the use of various small molecule inhibitors to induce cell death and mimic in vivo cell death during transplantation can be considered a limitation. Inducing cell death through drugs is an artificial model compared to changing cellular conditions to mimic ischemia such as depriving the endothelial cells of oxygen through hypoxia.

#### 4.4 Conclusion and Study Significance

In this study, we were able to build upon our knowledge from the previous studies completed in the group and provided evidence that AIF plays a role in endothelial cell death at acidic pH conditions and that these pH conditions may control for the activation of specific cell death pathways.

While specifically AIF deletion did not produce a reduction in cell death at low pH, it is possible that targeting upstream regulators of AIF may yield protection against cell death in organ transplantation. The main goal of this study was to develop a better understanding of end-stage mechanisms involving AIF at acidic conditions. In defining the mechanisms involved in these cell death pathways, potential pharmacological agents

could be used to block these routes and ultimately enhance the preservation of organs or expand eligibility criteria, thus addressing donor organ shortages<sup>7,39</sup>. Considering the cell death mechanism of necroptosis at pH 7.4 differed from pH 6.5, our study suggests that a comprehensive therapy should separately treat ischemia and reperfusion respectively.

## References

1. Metra, M. & Teerlink, J. R. Heart failure. *The Lancet* **390**, 1981–1995 (2017).
2. Ziaeeian, B. & Fonarow, G. C. Epidemiology and aetiology of heart failure. *Nature Reviews Cardiology* **13**, 368–378 (2016).
3. Murphy, S. P., Ibrahim, N. E. & Januzzi, J. L. Heart Failure With Reduced Ejection Fraction. *JAMA* **324**, 488 (2020).
4. Lippi, G. & Sanchis-Gomar, F. Global epidemiology and future trends of heart failure. *AME Medical Journal* **5**, 15–15 (2020).
5. Tonsho, M., Michel, S., Ahmed, Z., Alessandrini, A. & Madsen, J. C. Heart transplantation: challenges facing the field. *Cold Spring Harb Perspect Med* **4**, (2014).
6. Gupta, T. & Krim, S. R. Cardiac Transplantation: Update on a Road Less Traveled. *Ochsner Journal* **19**, 369–377 (2019).
7. Scheuer, S. E., Jansz, P. C. & Macdonald, P. S. Heart transplantation following donation after circulatory death: Expanding the donor pool. *The Journal of Heart and Lung Transplantation* **40**, 882–889 (2021).
8. Redd, M. A. *et al.* Therapeutic Inhibition of Acid-Sensing Ion Channel 1a Recovers Heart Function After Ischemia–Reperfusion Injury. *Circulation* **144**, 947–960 (2021).
9. Colvin, M. M. *et al.* Sensitization in Heart Transplantation: Emerging Knowledge: A Scientific Statement From the American Heart Association. *Circulation* **139**, (2019).
10. Stehlik, J., Kobashigawa, J., Hunt, S. A., Reichenspurner, H. & Kirklin, J. K. Honoring 50 Years of Clinical Heart Transplantation in Circulation. *Circulation* **137**, 71–87 (2018).

11. Tang, P. C. *et al.* Risk factors for heart transplant survival with greater than 5 h of donor heart ischemic time. *Journal of Cardiac Surgery* **36**, 2677–2684 (2021).
12. McCartney, S. L., Patel, C. & del Rio, J. M. Long-term outcomes and management of the heart transplant recipient. *Best Practice & Research Clinical Anaesthesiology* **31**, 237–248 (2017).
13. Singh, S. S. A., Dalzell, J. R., Berry, C. & Al-Attar, N. Primary graft dysfunction after heart transplantation: a thorn amongst the roses. *Heart Fail Rev* **24**, 805–820 (2019).
14. Squiers, J. J. *et al.* Long-term outcomes of patients with primary graft dysfunction after cardiac transplantation. *European Journal of Cardio-Thoracic Surgery* **60**, 1178–1183 (2021).
15. Awad, M. *et al.* Early Denervation and Later Reinnervation of the Heart Following Cardiac Transplantation: A Review. *J Am Heart Assoc* **5**, (2016).
16. Kaczorowski, D. J., Datta, J., Kamoun, M., Dries, D. L. & Woo, Y. J. Profound hyperacute cardiac allograft rejection rescue with biventricular mechanical circulatory support and plasmapheresis, intravenous immunoglobulin, and rituximab therapy. *Journal of Cardiothoracic Surgery* **8**, 48 (2013).
17. Duncan, M. D. & Wilkes, D. S. Transplant-related immunosuppression: a review of immunosuppression and pulmonary infections. *Proc Am Thorac Soc* **2**, 449–55 (2005).
18. Urschel, S. & West, L. J. ABO-Incompatible Heart Transplantation. *Curr Opin Pediatr* **28**, 613–9 (2016).
19. West, L. J. *et al.* ABO-Incompatible Heart Transplantation in Infants. *New England Journal of Medicine* **344**, 793–800 (2001).
20. Ingulli, E. Mechanism of cellular rejection in transplantation. *Pediatric Nephrology (Berlin, Germany)* **25**, 61–74 (2010).

21. Hurskainen, M., Ainasoja, O. & Lemström, K. B. Failing Heart Transplants and Rejection—A Cellular Perspective. *Journal of Cardiovascular Development and Disease* **8**, 180 (2021).
22. Colvin, M. M. *et al.* Antibody-Mediated Rejection in Cardiac Transplantation: Emerging Knowledge in Diagnosis and Management. *Circulation* **131**, 1608–1639 (2015).
23. Thrush, P. T., Urschel, S. & Pahl, E. Posttransplant Heart Failure. *Heart Failure in the Child and Young Adult: From Bench to Bedside* 625–638 (2018) doi:10.1016/B978-0-12-802393-8.00047-8.
24. Chih, S. *et al.* Antibody-mediated rejection: an evolving entity in heart transplantation. *J Transplant* **2012**, 210210 (2012).
25. Pober, J. S., Chih, S., Kobashigawa, J., Madsen, J. C. & Tellides, G. Cardiac allograft vasculopathy: current review and future research directions. *Cardiovascular Research* (2021) doi:10.1093/cvr/cvab259.
26. Weis, M. & Cooke, J. P. Cardiac Allograft Vasculopathy and Dysregulation of the NO Synthase Pathway. *Arteriosclerosis, Thrombosis, and Vascular Biology* **23**, 567–575 (2003).
27. Sciaccaluga, C. *et al.* The role of non-invasive imaging modalities in cardiac allograft vasculopathy: an updated focus on current evidences. *Heart Failure Reviews* **27**, 1235–1246 (2022).
28. Ramzy, D. *et al.* Cardiac allograft vasculopathy: a review. *Can J Surg* **48**, 319–27 (2005).
29. Ortega-Legaspi, J. M. & Bravo, P. E. Diagnosis and management of cardiac allograft vasculopathy. *Heart* **108**, 586 (2022).

30. Alba, A. C. Complications after Heart Transplantation: Hope for the Best, but Prepare for the Worst. *International Journal of Transplantation Research and Medicine* **2**, (2016).
31. Shen, B. *et al.* Current Status of Malignant Tumors after Organ Transplantation. *Biomed Res Int* **2022**, 5852451 (2022).
32. Fujioka, S. *et al.* NF-kappaB and AP-1 connection: mechanism of NF-kappaB-dependent regulation of AP-1 activity. *Mol Cell Biol* **24**, 7806–19 (2004).
33. Cowled, P. & Fitridge, R. *Pathophysiology of Reperfusion Injury*. (2011).
34. Fernández, A. R., Sánchez-Tarjuelo, R., Cravedi, P., Ochando, J. & López-Hoyos, M. Review: Ischemia Reperfusion Injury—A Translational Perspective in Organ Transplantation. *International Journal of Molecular Sciences* **21**, 8549 (2020).
35. Zhu, C. *et al.* Supplementing preservation solution with mitochondria-targeted H<sub>2</sub>S donor AP39 protects cardiac grafts from prolonged cold ischemia–reperfusion injury in heart transplantation. *American Journal of Transplantation* **19**, 3139–3148 (2019).
36. Banner, N. R. *et al.* The Importance of Cold and Warm Cardiac Ischemia for Survival After Heart Transplantation. *Transplantation* **86**, 542–547 (2008).
37. Jernryd, V., Metzsch, C., Andersson, B. & Nilsson, J. The influence of ischemia and reperfusion time on outcome in heart transplantation. *Clinical Transplantation* **34**, (2020).
38. Reich, H. J. *et al.* Effects of Older Donor Age and Cold Ischemic Time on Long-Term Outcomes of Heart Transplantation. *Texas Heart Institute Journal* **45**, 17–22 (2018).
39. Russo, M. J. *et al.* The effect of ischemic time on survival after heart transplantation varies by donor age: An analysis of the United Network for Organ

- Sharing database. *The Journal of Thoracic and Cardiovascular Surgery* **133**, 554–559 (2007).
40. Patel, P. M. *et al.* Minimizing Ischemia Reperfusion Injury in Xenotransplantation. *Frontiers in Immunology* **12**, (2021).
  41. Wong, B. W., Marsch, E., Treps, L., Baes, M. & Carmeliet, P. Endothelial cell metabolism in health and disease: impact of hypoxia. *The EMBO Journal* **36**, 2187–2203 (2017).
  42. Slegtenhorst, B. R., Dor, F. J. M. F., Rodriguez, H., Voskuil, F. J. & Tullius, S. G. Ischemia/Reperfusion Injury and its Consequences on Immunity and Inflammation. *Current Transplantation Reports* **1**, 147–154 (2014).
  43. Chen, S. & Li, S. The Na<sup>+</sup>/Ca<sup>2+</sup> exchanger in cardiac ischemia/reperfusion injury. *Medical Science Monitor* **18**, RA161–RA165 (2012).
  44. Park, C.-O., Xiao, X.-H. & Allen, D. G. Changes in intracellular Na<sup>+</sup> and pH in rat heart during ischemia: role of Na<sup>+</sup>/H<sup>+</sup> exchanger. *American Journal of Physiology-Heart and Circulatory Physiology* **276**, H1581–H1590 (1999).
  45. Steenbergen, C., Deleeuw, G., Rich, T. & Williamson, J. R. Effects of acidosis and ischemia on contractility and intracellular pH of rat heart. *Circulation Research* **41**, 849–858 (1977).
  46. Zhang, Z. X. *et al.* Intracellular pH Regulates TRAIL-Induced Apoptosis and Necroptosis in Endothelial Cells. *Journal of Immunology Research* **2017**, (2017).
  47. Kalogeris, T., Baines, C. P., Krenz, M. & Korthuis, R. J. Cell Biology of Ischemia/Reperfusion Injury. *International Review of Cell and Molecular Biology* **298**, 229–317 (2012).
  48. Soares, R. O. S., Losada, D. M., Jordani, M. C., Évora, P. & Castro-E-Silva, O. Ischemia/Reperfusion Injury Revisited: An Overview of the Latest Pharmacological Strategies. *Int J Mol Sci* **20**, (2019).

49. Wu, M.-Y. *et al.* Current Mechanistic Concepts in Ischemia and Reperfusion Injury. *Cellular Physiology and Biochemistry* **46**, 1650–1667 (2018).
50. Xiang, M. *et al.* Role of Oxidative Stress in Reperfusion following Myocardial Ischemia and Its Treatments. *Oxidative Medicine and Cellular Longevity* **2021**, 1–23 (2021).
51. Silvis, M. J. M. *et al.* Damage-Associated Molecular Patterns in Myocardial Infarction and Heart Transplantation: The Road to Translational Success. *Frontiers in Immunology* **11**, (2020).
52. Tran, D. T. *et al.* Impact of Mitochondrial Permeability on Endothelial Cell Immunogenicity in Transplantation. *Transplantation* **102**, 935–944 (2018).
53. Marcu, R. *et al.* The Mitochondrial Permeability Transition Pore Regulates Endothelial Bioenergetics and Angiogenesis. *Circulation Research* **116**, 1336–1345 (2015).
54. Halestrap, A. Mitochondrial permeability transition pore opening during myocardial reperfusion—a target for cardioprotection. *Cardiovascular Research* **61**, 372–385 (2004).
55. Arumugam, T. v. *et al.* Toll-Like Receptors in Ischemia-Reperfusion Injury. *Shock* **32**, 4–16 (2009).
56. Lukenaite, B. *et al.* Necroptosis in Solid Organ Transplantation: A Literature Overview. *International Journal of Molecular Sciences* **23**, 3677 (2022).
57. Alem, M. M. Endothelial Dysfunction in Chronic Heart Failure: Assessment, Findings, Significance, and Potential Therapeutic Targets. *International Journal of Molecular Sciences* **20**, (2019).
58. Kozanoglu, I. & Pepedil-Tanrikulu, F. Functions of the endothelium and its role in hematopoietic cell transplantation. *Transfusion and Apheresis Science* **61**, 103368 (2022).



59. Talman, V. & Kivelä, R. Cardiomyocyte-Endothelial Cell Interactions in Cardiac Remodeling and Regeneration. *Front Cardiovasc Med* **5**, 101 (2018).
60. Crimi, E. *et al.* Effects of intracellular acidosis on endothelial function: An overview. *Journal of Critical Care* **27**, 108–118 (2012).
61. Giannitsi, S., Bougiakli, M., Bechlioulis, A. & Naka, K. Endothelial dysfunction and heart failure: A review of the existing bibliography with emphasis on flow mediated dilation. *JRSM Cardiovascular Disease* **8**, 1–7 (2019).
62. Zuchi, C. *et al.* Role of endothelial dysfunction in heart failure. *Heart Failure Reviews* **25**, 21–30 (2020).
63. Marti, C. N. *et al.* Endothelial Dysfunction, Arterial Stiffness, and Heart Failure. *J Am Coll Cardiol* **60**, 1455–1469 (2012).
64. Kummer, L. *et al.* Vascular Signaling in Allogenic Solid Organ Transplantation – The Role of Endothelial Cells. *Frontiers in Physiology* **11**, (2020).
65. Peelen, D. M., Hoogduijn, M. J., Hesselink, D. A. & Baan, C. C. Advanced in vitro Research Models to Study the Role of Endothelial Cells in Solid Organ Transplantation. *Frontiers in Immunology* **12**, (2021).
66. Hébert, M. J. & Jevnikar, A. M. The Impact of Regulated Cell Death Pathways on Alloimmune Responses and Graft Injury. *Current Transplantation Reports* **2**, (2015).
67. Elmore, S. Apoptosis: A Review of Programmed Cell Death. *Toxicologic Pathology* **35**, 495–516 (2007).
68. Linkermann, A. & Green, D. R. Necroptosis. *N Engl J Med* **370**, 455–65 (2014).
69. Li, W. *et al.* Ferroptotic cell death and TLR4/Trif signaling initiate neutrophil recruitment after heart transplantation. *J Clin Invest* **129**, 2293–2304 (2019).

70. Jia, C. *et al.* Endothelial cell pyroptosis plays an important role in Kawasaki disease via HMGB1/RAGE/cathepsin B signaling pathway and NLRP3 inflammasome activation. *Cell Death & Disease* **10**, 778 (2019).
71. Costello, J. P., Mohanakumar, T. & Nath, D. S. Mechanisms of chronic cardiac allograft rejection. *Tex Heart Inst J* **40**, 395–9 (2013).
72. Rifle, G., Mousson, C. & Hervé, P. Endothelial Cells in Organ Transplantation: Friends or Foes? *Transplantation* **82**, S4–S5 (2006).
73. Kummer, L. *et al.* Vascular Signaling in Allogenic Solid Organ Transplantation – The Role of Endothelial Cells. *Frontiers in Physiology* **11**, (2020).
74. Al-Lamki, R. S., Bradley, J. R. & Pober, J. S. Endothelial Cells in Allograft Rejection. *Transplantation* **86**, 1340–1348 (2008).
75. Miller, L. W., Granville, D. J., Narula, J. & McManus, B. M. Apoptosis in Cardiac Transplant Rejection. *Cardiology Clinics* **19**, 141–154 (2001).
76. Scarabelli, T. *et al.* Apoptosis of Endothelial Cells Precedes Myocyte Cell Apoptosis in Ischemia/Reperfusion Injury. *Circulation* **104**, 253–256 (2001).
77. Choi, M. E., Price, D. R., Ryter, S. W. & Choi, A. M. K. Necroptosis: A crucial pathogenic mediator of human disease. *JCI Insight* vol. 4 Preprint at <https://doi.org/10.1172/jci.insight.128834> (2019).
78. Loreto, C. *et al.* The role of intrinsic pathway in apoptosis activation and progression in Peyronie’s disease. *Biomed Res Int* **2014**, 616149 (2014).
79. Fulda, S. & Debatin, K.-M. Extrinsic versus intrinsic apoptosis pathways in anticancer chemotherapy. *Oncogene* **25**, 4798–4811 (2006).
80. Yuste, V. J. *et al.* Cysteine protease inhibition prevents mitochondrial apoptosis-inducing factor (AIF) release. *Cell Death & Differentiation* **12**, 1445–1448 (2005).

81. Wolf, B. B., Schuler, M., Echeverri, F. & Green, D. R. Caspase-3 Is the Primary Activator of Apoptotic DNA Fragmentation via DNA Fragmentation Factor-45/Inhibitor of Caspase-activated DNase Inactivation. *Journal of Biological Chemistry* **274**, 30651–30656 (1999).
82. Tonnus, W. *et al.* The pathological features of regulated necrosis. *The Journal of Pathology* **247**, 697–707 (2019).
83. Liu, X. *et al.* The role of necroptosis in disease and treatment. *MedComm (Beijing)* **2**, 730–755 (2021).
84. Takahashi, N. *et al.* Necrostatin-1 analogues: critical issues on the specificity, activity and in vivo use in experimental disease models. *Cell Death & Disease* **3**, e437–e437 (2012).
85. Conrad, M., Angeli, J. P. F., Vandenabeele, P. & Stockwell, B. R. Regulated necrosis: disease relevance and therapeutic opportunities. *Nature Reviews Drug Discovery* **15**, 348–366 (2016).
86. Galluzzi, L., Kepp, O., Chan, F. K.-M. & Kroemer, G. Necroptosis: Mechanisms and Relevance to Disease. *Annual Review of Pathology: Mechanisms of Disease* **12**, 103–130 (2017).
87. He, S. & Wang, X. RIP kinases as modulators of inflammation and immunity. *Nature Immunology* **19**, 912–922 (2018).
88. Weinlich, R., Oberst, A., Beere, H. M. & Green, D. R. Necroptosis in development, inflammation and disease. *Nature Reviews Molecular Cell Biology* **18**, 127–136 (2017).
89. Kaczmarek, A., Vandenabeele, P. & Krysko, D. V. Necroptosis: The Release of Damage-Associated Molecular Patterns and Its Physiological Relevance. *Immunity* **38**, 209–223 (2013).

90. Orozco, S. & Oberst, A. RIPK3 in cell death and inflammation: the good, the bad, and the ugly. *Immunol Rev* **277**, 102–112 (2017).
91. Zhdanov, D. D. *et al.* Regulation of Apoptotic Endonucleases by EndoG. *DNA Cell Biol* **34**, 316–26 (2015).
92. Nagata, S., Nagase, H., Kawane, K., Mukae, N. & Fukuyama, H. Degradation of chromosomal DNA during apoptosis. *Cell Death and Differentiation* **10**, 108–116 (2003).
93. Linkermann, A. *et al.* Two independent pathways of regulated necrosis mediate ischemia-reperfusion injury. *Proc Natl Acad Sci U S A* **110**, 12024–9 (2013).
94. Tang, Y. *et al.* Linear ubiquitination of cFLIP induced by LUBAC contributes to TNF $\alpha$ -induced apoptosis. *J Biol Chem* **293**, 20062–20072 (2018).
95. Kluge, M. A., Fetterman, J. L. & Vita, J. A. Mitochondria and Endothelial Function. *Circulation Research* **112**, 1171–1188 (2013).
96. Cai, Z. & Liu, Z.-G. Execution of RIPK3-regulated necrosis. *Molecular & Cellular Oncology* **1**, e960759 (2014).
97. Delavallée, L., Cabon, L., Galán-Malo, P., Lorenzo, H. K. & Susin, S. A. AIF-mediated caspase-independent necroptosis: A new chance for targeted therapeutics. *IUBMB Life* **63**, 221–232 (2011).
98. Baritaud, M. *et al.* AIF-mediated caspase-independent necroptosis requires ATM and DNA-PK-induced histone H2AX Ser139 phosphorylation. *Cell Death & Disease* **3**, e390–e390 (2012).
99. Benítez-Guzmán, A., Arriaga-Pizano, L., Morán, J. & Gutiérrez-Pabello, J. A. Endonuclease G takes part in AIF-mediated caspase-independent apoptosis in *Mycobacterium bovis*-infected bovine macrophages. *Veterinary Research* **49**, 69 (2018).

100. Jiang, X., Stockwell, B. R. & Conrad, M. Ferroptosis: mechanisms, biology and role in disease. *Nature Reviews Molecular Cell Biology* **22**, 266–282 (2021).
101. Yuan, W. *et al.* The role of ferroptosis in endothelial cell dysfunction. *Cell Cycle* 1–18 (2022) doi:10.1080/15384101.2022.2079054.
102. Ren, J. X. *et al.* Crosstalk between Oxidative Stress and Ferroptosis/Oxytosis in Ischemic Stroke: Possible Targets and Molecular Mechanisms. *Oxidative Medicine and Cellular Longevity* vol. 2021 Preprint at <https://doi.org/10.1155/2021/6643382> (2021).
103. Xie, Y. *et al.* Ferroptosis: process and function. *Cell Death & Differentiation* **23**, 369–379 (2016).
104. Tan, S., Schubert, D. & Maher, P. Oxytosis: A novel form of programmed cell death. *Curr Top Med Chem* **1**, (2001).
105. Ray Chaudhuri, A. & Nussenzweig, A. The multifaceted roles of PARP1 in DNA repair and chromatin remodelling. *Nature Reviews Molecular Cell Biology* **18**, 610–621 (2017).
106. Mashimo, M. *et al.* The 89-kDa PARP1 cleavage fragment serves as a cytoplasmic PAR carrier to induce AIF-mediated apoptosis. *Journal of Biological Chemistry* **296**, (2021).
107. Wang, Y. *et al.* A nuclease that mediates cell death induced by DNA damage and poly(ADP-ribose) polymerase-1. *Science (1979)* **354**, (2016).
108. Sosna, J. *et al.* TNF-induced necroptosis and PARP-1-mediated necrosis represent distinct routes to programmed necrotic cell death. *Cell Mol Life Sci* **71**, 331–48 (2014).
109. Wang, H., Shimoji, M., Yu, S.-W., Dawson, T. M. & Dawson, V. L. Apoptosis Inducing Factor and PARP-Mediated Injury in the MPTP Mouse Model of Parkinson's Disease. *Ann N Y Acad Sci* **991**, 132–139 (2006).

110. Cheung, E. C. C. *et al.* Apoptosis-inducing factor is a key factor in neuronal cell death propagated by BAX-dependent and BAX-independent mechanisms. *J Neurosci* **25**, 1324–34 (2005).
111. Stambolsky, P. *et al.* Regulation of AIF expression by p53. *Cell Death & Differentiation* **13**, 2140–2149 (2006).
112. Lemasters, J. J. Cytolethality. *Comprehensive Toxicology: Second Edition* **1–14**, 245–268 (2010).
113. Park, H. *et al.* PAAN/MIF nuclease inhibition prevents neurodegeneration in Parkinson's disease. *Cell* **185**, 1943-1959.e21 (2022).
114. Andelova, N., Waczulikova, I., Talian, I., Sykora, M. & Ferko, M. mPTP Proteins Regulated by Streptozotocin-Induced Diabetes Mellitus Are Effectively Involved in the Processes of Maintaining Myocardial Metabolic Adaptation. *Int J Mol Sci* **21**, (2020).
115. Perrelli, M.-G., Pagliaro, P. & Penna, C. Ischemia/reperfusion injury and cardioprotective mechanisms: Role of mitochondria and reactive oxygen species. *World Journal of Cardiology* **3**, 186–200 (2011).
116. Norberg, E., Orrenius, S. & Zhivotovsky, B. Mitochondrial regulation of cell death: Processing of apoptosis-inducing factor (AIF). *Biochemical and Biophysical Research Communications* **396**, 95–100 (2010).
117. Doti, N. *et al.* Inhibition of the AIF/CypA complex protects against intrinsic death pathways induced by oxidative stress. *Cell Death Dis* **5**, e993 (2014).
118. Susin, S. A. *et al.* Molecular characterization of mitochondrial apoptosis-inducing factor. *Nature* **397**, 441–446 (1999).
119. Zhu, C. *et al.* Apoptosis-inducing factor is a major contributor to neuronal loss induced by neonatal cerebral hypoxia-ischemia. *Cell Death & Differentiation* **14**, 775–784 (2007).

120. Herrmann, J. M. & Riemer, J. Apoptosis inducing factor and mitochondrial NADH dehydrogenases: redox-controlled gear boxes to switch between mitochondrial biogenesis and cell death. *Biological Chemistry* **402**, 289–297 (2021).
121. Sevrioukova, I. F. Apoptosis-inducing factor: structure, function, and redox regulation. *Antioxid Redox Signal* **14**, 2545–79 (2011).
122. Millan, A. & Huerta, S. Apoptosis-Inducing Factor and Colon Cancer. *Journal of Surgical Research* **151**, 163–170 (2009).
123. Chen, Q., Szczepanek, K., Hu, Y., Thompson, J. & Lesnfsky, E. J. A deficiency of apoptosis inducing factor (AIF) in Harlequin mouse heart mitochondria paradoxically reduces ROS generation during ischemia-reperfusion. *Front Physiol* **5**, 271 (2014).
124. Bano, D. & Prehn, J. H. M. Apoptosis-Inducing Factor (AIF) in Physiology and Disease: The Tale of a Repented Natural Born Killer. *EBioMedicine* **30**, 29–37 (2018).
125. Baritaud, M., Boujrad, H., Lorenzo, H. K., Krantic, S. & Susin, S. A. Histone H2AX: The missing link in AIF-mediated caspase-independent programmed necrosis. *Cell Cycle* **9**, 3186–3193 (2010).
126. Modjtahedi, N., Giordanetto, F., Madeo, F. & Kroemer, G. Apoptosis-inducing factor: vital and lethal. *Trends in Cell Biology* **16**, 264–272 (2006).
127. Artus, C. *et al.* AIF promotes chromatinolysis and caspase-independent programmed necrosis by interacting with histone H2AX. *The EMBO Journal* **29**, 1585–1599 (2010).
128. Ravagnan, L. *et al.* Heat-shock protein 70 antagonizes apoptosis-inducing factor. *Nature Cell Biology* **3**, 839–843 (2001).
129. Yang, S., Huang, J., Liu, P., Li, J. & Zhao, S. Apoptosis-inducing factor (AIF) nuclear translocation mediated caspase-independent mechanism involves in X-ray-

- induced MCF-7 cell death. *International Journal of Radiation Biology* **93**, 270–278 (2017).
130. Candé, C., Vahsen, N., Garrido, C. & Kroemer, G. Apoptosis-inducing factor (AIF): caspase-independent after all. *Cell Death & Differentiation* **11**, 591–595 (2004).
131. Pavlosky, A. *et al.* RIPK3-mediated necroptosis regulates cardiac allograft rejection. *American Journal of Transplantation* **14**, 1778–1790 (2014).
132. Qamar, A. *et al.* Cyclophilin D Regulates the Nuclear Translocation of AIF, Cardiac Endothelial Cell Necroptosis and Murine Cardiac Transplant Injury. *International Journal of Molecular Sciences* **22**, (2021).
133. Pantazi, E., Bejaoui, M., Folch-Puy, E., Adam, R. & Roselló-Catafau, J. Advances in treatment strategies for ischemia reperfusion injury. *Expert Opinion on Pharmacotherapy* **17**, 169–179 (2016).
134. Gorodetsky, A. A., Kirilyuk, I. A., Khramtsov, V. v. & Komarov, D. A. Functional electron paramagnetic resonance imaging of ischemic rat heart: Monitoring of tissue oxygenation and pH. *Magnetic Resonance in Medicine* **76**, 350–358 (2016).
135. Gabel, S. A., Cross, H. R., London, R. E., Steenbergen, C. & Murphy, E. Decreased intracellular pH is not due to increased H<sup>+</sup> extrusion in preconditioned rat hearts. *American Journal of Physiology-Heart and Circulatory Physiology* **273**, H2257–H2262 (1997).
136. Du, C., Fang, M., Li, Y., Li, L. & Wang, X. Smac, a Mitochondrial Protein that Promotes Cytochrome c-Dependent Caspase Activation by Eliminating IAP Inhibition. *Cell* **102**, 33–42 (2000).
137. Adrain, C., Creagh, E. M. & Martin, S. J. Apoptosis-associated release of Smac/DIABLO from mitochondria requires active caspases and is blocked by Bcl-2. *EMBO J* **20**, 6627–36 (2001).



138. Micheau, O. & Tschopp, J. Induction of TNF Receptor I-Mediated Apoptosis via Two Sequential Signaling Complexes. *Cell* **114**, 181–190 (2003).
139. Quarato, G. *et al.* The cyclophilin inhibitor alisporivir prevents hepatitis C virus-mediated mitochondrial dysfunction. *Hepatology* **55**, 1333–1343 (2012).
140. Zhu, C. *et al.* Cyclophilin A participates in the nuclear translocation of apoptosis-inducing factor in neurons after cerebral hypoxia-ischemia. *J Exp Med* **204**, 1741–8 (2007).
141. Farina, B. *et al.* Structural and biochemical insights of CypA and AIF interaction. *Scientific Reports* **7**, 1138 (2017).
142. Gan, I. *et al.* Mitochondrial permeability regulates cardiac endothelial cell necroptosis and cardiac allograft rejection. *American Journal of Transplantation* **19**, 686–698 (2019).
143. Kwok, C. *et al.* Necroptosis Is Involved in CD4+ T Cell-Mediated Microvascular Endothelial Cell Death and Chronic Cardiac Allograft Rejection. *Transplantation* **101**, 2026–2037 (2017).
144. Kupiec-Weglinski, J. W. Grand Challenges in Organ Transplantation. *Frontiers in Transplantation* **1**, (2022).
145. Sharma, V., Kaur, R., Bhatnagar, A. & Kaur, J. Low-pH-induced apoptosis: role of endoplasmic reticulum stress-induced calcium permeability and mitochondria-dependent signaling. *Cell Stress and Chaperones* **20**, 431–440 (2015).
146. Kittl, M. *et al.* Low pH Attenuates Apoptosis by Suppressing the Volume-Sensitive Outwardly Rectifying (VSOR) Chloride Current in Chondrocytes. *Frontiers in Cell and Developmental Biology* **9**, (2022).
147. Meurette, O. *et al.* TRAIL Induces Receptor-Interacting Protein 1–Dependent and Caspase-Dependent Necrosis-Like Cell Death under Acidic Extracellular Conditions. *Cancer Research* **67**, 218–226 (2007).

148. Zhang, W., Fan, W., Guo, J. & Wang, X. Osmotic stress activates RIPK3/MLKL-mediated necroptosis by increasing cytosolic pH through a plasma membrane Na<sup>+</sup>/H<sup>+</sup> exchanger. *Science Signaling* **15**, (2022).
149. Wang, Y.-Z. *et al.* Tissue acidosis induces neuronal necroptosis via ASIC1a channel independent of its ionic conduction. *Elife* **4**, (2015).
150. Moriwaki, K., Balaji, S. & Ka-Ming Chan, F. The death-inducing activity of RIPK1 is regulated by the pH environment. *Science Signaling* **13**, (2020).
151. Milasta, S. *et al.* Apoptosis-Inducing-Factor-Dependent Mitochondrial Function Is Required for T Cell but Not B Cell Function. *Immunity* **44**, 88–102 (2016).

## Curriculum Vitae

**Name:** Laura Xu

**Post-secondary  
Education and  
Degrees:** McMaster University  
Hamilton, Ontario, Canada  
2016-2020 B.H.Sc.

The University of Western Ontario  
London, Ontario, Canada  
2020-2022 M.Sc.

### Conference Presentations:

**Abstract:** *Mechanism of AIF-Regulated Nuclei Damage.* **Laura Xu**, Patrick McLeod, Zhu-Xu Zhang.

- Department of Medicine Resident Research Day, London, Ontario, May 28, 2021.
- Pathology and Laboratory Medicine Research Day, London, Ontario, April 7, 2021.

**Abstract:** *Acidic pH Environment Alters Cell Death and Regulates AIF Translocation in Endothelial Cells.* **Laura Xu**, Patrick McLeod, Xuyan Huang, Haitao Lu, Zhu-Xu Zhang.

- Pathology and Laboratory Medicine Research Day, London, Ontario, March 31, 2022.
- Department of Medicine Resident Research Day, London, Ontario, May 20, 2022.
- London Health Research Day, London, Ontario, May 31, 2022.

### Publications:

Qamar A., Zhao J., **Xu L.**, et al. (2021). Cyclophilin D Regulates the Nuclear Translocation of AIF, Cardiac Endothelial Cell Necroptosis and Murine Cardiac Transplant Injury. *International Journal of Molecular Sciences*, 22(20), 11038.